

## **Main revisions and response to reviewers' comments**

**Manuscript No.:** acp-2016-540

**Title:** A high-resolution regional emission inventory of atmospheric mercury and its comparison with multi-scale inventories: a case study of Jiangsu, China

**Authors:** Hui Zhong, Yu Zhao, Marilena Muntean, Lei Zhang, Jie Zhang

We thank very much for the valuable comments from the two reviewers, which help us improve the quality of our manuscript. The comments were carefully considered and revisions have been made in response to the comments and suggestion. The major revisions were marked in red bold in the submitted manuscript. Our responses to each comment or suggestion are provided in details as below, along with the brief description on the revision actions taken in the revised manuscript.

### **Reviewer #1**

The article presents a comparison of international, national and a new local bottom-up Hg emission inventory for the Jiangsu region in China. The study highlights the serious discrepancies, in both emission totals and speciation, between emission inventory estimates. This has serious implications for the regional atmospheric Hg burden and deposition flux. If the underestimate for Jiangsu is representative for the major economies of the region then this would have global repercussions.

### **Response and revisions:**

We appreciate the reviewer's positive remarks.

Q1. Unfortunately the authors do not comment on how wide-spread the underestimations in Hg emissions they have identified for Jiangsu may be. Are the

shortcomings in the national and global inventories identified for Jiangsu applicable to other heavily industrialised regions of China? It would improve the article if the authors could provide estimates of the possible range of underestimation of Chinese emissions and how this would influence the global Hg emissions total.

**Response and revisions:**

We thank the reviewer's important comment. Through the comparisons between provincial and other downscaled global/national inventories, it could be found that cement and iron & steel industries were the two most important sectors of which the Hg emissions were significantly underestimated by previous inventories. The underestimations came mainly from the ignorance of high Hg release ratio of precalciner technology with dust recycling, and/or application of relatively low emission factors for steel production. For example, the estimation of CEM and ISP emissions by the national inventory (Zhao et al., 2015a) was 77% lower than the provincial one, and the difference accounted for 30% of the total anthropogenic Hg emissions from the provincial inventory. Compared to the provincial inventory, for example, we could thus cautiously infer that Hg emissions might also be underestimated for other regions with intensive cement and steel industries in China in previous inventories. For other big sources, e.g., power plants and industrial boilers, the Hg emissions were influenced largely by the Hg contents in coal and the application of emission control devices. Whether the emissions of those sources were underestimated or not for other parts of the country could hardly be judged unless detailed information gets available for the regions. In general, however, the method developed and demonstrated for Jiangsu in this work could be promoted to other provinces, particularly for those with intensive industrial plants. With the detailed data on individual sources sufficiently applied, the accuracy in China's Hg emission estimation can be expected to be largely improved.

We presented the discussions **in lines 666-682, Page 22 at the end of the revised manuscript.**

Q2. The difference in Hg emission speciation (and to a lesser extent emission height) between the inventories will have an impact on local deposition and Hg export estimates from the region, neither of these aspects are discussed in any detail.

**Response and revisions:**

We thank the reviewer's comment. Relevant discussions have been added **in lines 576-581, Page 19 at the end of Section 3.3 in the revised manuscript:**

The smaller fraction of Hg emissions under 150m and larger fraction of Hg<sup>2+</sup> as discussed in Section 3.2 in the provincial inventory are expected to result in more local deposition and less long-range transport compared to previous inventories when they are applied in CTM. The re-emissions of legacy Hg could then be enhanced and make a significant contribution to atmospheric Hg concentrations, as indicated by Zhu et al. (2012).

Q3. The description of the database compilation is thorough but rather repetitive of previous work. The English requires substantial improvement and overall the manuscript could be more concise.

**Response and revisions:**

We thank the reviewer's comment. The description of the database compilation is given in Section 2.3, and databases for Hg emission factors/related parameters are provided in the supplement avoiding unnecessary description. We have also tried our best to shorten the manuscript and to make it more concise.

Q4. Collaboration with modelling groups or at least performing some trajectory calculations with the previous and revised speciation would make the paper far more interesting.

**Response and revisions:**

We thank the reviewer's important comment. We agree that chemistry transport modeling (CTM) is a very crucial step to evaluate the emission inventory, and it is

exactly what we are working on. We are currently conducting the Hg simulation at provincial scale with WRF-CMAQ-Hg, using the different inventories mentioned in this paper. The improvement in revised provincial inventory is expected to be evaluated by comparing the model performances with various inventories. We hope the work could be finished and a companion paper would come out soon.

Q5. Making the emissions database available would seem a good idea as I am sure it would lead to fruitful joint research beneficial not only to the science community but also to local environmental agencies and policy makers. The fact that some of the data sources are not publicly available is a concern.

**Response and revisions:**

We thank the reviewer's reminder and totally agree. We will upload the data to the website of our group. The data will be available online soon at <http://www.airqualitynju.com/En/Default>. We have stated this at the end of the revised manuscript.

Q6. Sections 2.1 and 2.2 could be shortened with reference to Sections 2.1 and 2.3 of Zhao et al., 2015 (Evaluating the effects of China's pollution controls on inter-annual trends and uncertainties of atmospheric mercury emissions, Atmos. Chem. Phys., 15, 4317-4337), which are very similar.

**Response and revisions:**

We thank the reviewer's comment and have tried to shorten the sections. For example, **in lines 188-189, Page 7 in the revised manuscript**, we have stated:

Activity data for MSWI, RSWI and BIO are taken following Zhao et al. (2015a).

It should be noted, however, that the provincial inventory is established with a bottom-up method, which is quite different from the approach by Zhao et al. (2015a). Thus some details in the provincial inventory approach must be given to avoid confusion.

Q7. Section 2.3, is this really a sensitivity analysis, or more simply an analysis of the scale of the differences in emissions which result from the assumptions made in the compilation of the inventories?

**Response and revisions:**

We thank the reviewer's comment. We agree with the reviewer that the analysis here is to quantify the scale of emission changes resulting from varied values of given parameters in different inventories. In the analysis, we include both the differences in assumptions for key parameters and the scale of corresponding emission changes due to the varied assumptions. We mean the analysis can thus show the sensitivity of the emissions to specific parameter.

Q8. Section 3.1.2 particularly is rather long and full of acronyms, it would likely aid the reader if it were divided into subsections.

**Response and revisions:**

We thank the reviewer's comment. Now the original Section 3.1.2 was divided into two sections, Section 3.1.2 for power plants and industrial boilers, and 3.1.3 for cement and iron & steel industries.

Q9. Section 3.3 would also benefit from being more concise.

**Response and revisions:**

We thank the reviewer's comment and have tried our best to shorten the section.

**Reviewer #2**

In this study, the authors developed a high-resolution Hg emission inventory of anthropogenic origin for 2010. The provincial inventory was compared to selected global and national inventories. Discrepancies in emission levels, speciation, and spatial distributions are evaluated. The major contribution of the study is comparison

of the inventories, and identifying the effects of different approaches and data on developing the inventories. The study is relevant since there are considerable information gaps between multi-scale inventories. The differences attribute mainly to the data of different sources and levels of details. A bottom-up approach used in this study could help improve the precision of the inventory.

**Response and revisions:**

We appreciate the reviewer's positive remarks.

Q1. A key question is, the authors indicated that part of the data are internal data from Environmental Protection Agency of Jiangsu Province, and the internal industry reports. We would like to see more explanations on these "internal data". (Line 128-131, could you provide more information on the PSC? Any difference between PSC and published statistical data? Line 180, please explain the internal industry reports.)

**Response and revisions:**

Pollution Source Census (PSC) was conducted by local environmental protection agencies, in which the data for individual emission sources were collected and compiled through on-site investigation, including manufacturing technology, production level, energy consumption, fuel quality, and emission control device. Compared to the energy and economic statistics at sector level that were commonly used in global/national inventories, we believe the plant-by-plant PSC data could provide more detailed and accurate information on individual emission sources, particularly for power and industrial plants. Moreover, differences in total energy consumption and industrial production levels exist between the PSC data and the energy/economic statistics. For example, the coal consumption by CPP in PSC for Jiangsu 2010 was 6% larger than the provincial statistics.

Internal industry reports indicate the association commercial reports that provide the activity data of intentional Hg use. Rarely included in the national or provincial statistics, the data were collected at <http://www.askci.com/>.

We have included the information **in lines 128-138, Pages 5-6 and in lines 187-188, Page 7 in the revised manuscript**, respectively.

Q2. Line 78, “there are currently very few studies focusing on Hg at regional/local scales”. This is not true.

**Response and revisions:**

We thank the reviewer's reminder. The sentence was revised as “there are currently very few studies on Hg emissions at regional/local scales in China”, **in lines 77-78, Page 4 in the revised manuscript**.

Q3. It would be interesting if at the end of the manuscript, the authors might give some discussions on the possibility of overall underestimation of mercury inventory for China, not just for the province. That is to say, the same problems in other national inventories might happen in other provinces in China.

**Response and revisions:**

We thank the reviewer's important comment, and it is similar to Q1 from another reviewer. Through the comparisons between provincial and other downscaled global/national inventories, it could be found that cement and iron & steel industries were the two most important sectors of which the Hg emissions were significantly underestimated by previous inventories. The underestimations came mainly from the ignorance of high Hg release ratio of precalciner technology with dust recycling, and/or application of relatively low emission factors for steel production. For example, the estimation of CEM and ISP emissions by the national inventory (Zhao et al., 2015a) was 77% lower than the provincial one, and the difference accounted for 30% of the total anthropogenic Hg emissions from the provincial inventory. Compared to the provincial inventory, for example, we could thus cautiously infer that Hg emissions might also be underestimated for other regions with intensive cement and steel industries in China in previous inventories. For other big sources, e.g., power plants and industrial boilers, the Hg emissions were influenced largely by

the Hg contents in coal and the application of emission control devices. Whether the emissions of those sources were underestimated or not for other parts of the country could hardly be judged unless detailed information gets available for the regions. In general, however, the method developed and demonstrated for Jiangsu in this work could be promoted to other provinces, particularly for those with intensive industrial plants. With the detailed data on individual sources sufficiently applied, the accuracy in China's Hg emission estimation can be expected to be largely improved.

We presented the discussions **in lines 666-682, Page 22 at the end of the revised manuscript.**



# TITLE PAGE

## **A high-resolution regional emission inventory of atmospheric mercury and its comparison with multi-scale inventories: a case study of Jiangsu, China**

Hui Zhong<sup>1</sup>, Yu Zhao<sup>1,2\*</sup>, Marilena Muntean<sup>3</sup>, Lei Zhang<sup>4</sup>, Jie Zhang<sup>2,5</sup>

1. State Key Laboratory of Pollution Control & Resource Reuse and School of the Environment, Nanjing University, 163 Xianlin Ave., Nanjing, Jiangsu 210023, China
2. Jiangsu Collaborative Innovation Center of Atmospheric Environment and Equipment Technology (CICAEET), Nanjing University of Information Science & Technology, Jiangsu 210044, China
3. European Commission, Joint Research Centre, Institute for Environment and Sustainability, Air and Climate Unit, Via E. Fermi, Ispra, Italy
4. University of Washington-Bothell, 18115 Campus Way NE, Bothell, WA 98011, U.S.A.
5. Jiangsu Provincial Academy of Environmental Science, 176 North Jiangdong Rd., Nanjing, Jiangsu 210036, China

\* Corresponding author: Phone: 86-25-89680650; email: [yuzhao@nju.edu.cn](mailto:yuzhao@nju.edu.cn)

## ABSTRACT

1  
2 A better understanding of the discrepancies in multi-scale inventories could give  
3 an insight on their approaches and limitations, and provide indications for further  
4 improvements; international, national and plant-by-plant data are primarily obtained  
5 to compile those inventories. In this study we develop a high-resolution inventory of  
6 Hg emissions at  $0.05^\circ \times 0.05^\circ$  for Jiangsu China using a bottom-up approach and then  
7 compare the results with available global/national inventories. With detailed  
8 information on individual sources and the updated emission factors from field  
9 measurements, applied, the annual Hg emissions of anthropogenic origin in Jiangsu  
10 2010 are estimated at 39 105 kg, of which 51%, 47% and 2% were  $\text{Hg}^0$ ,  $\text{Hg}^{2+}$ , and  
11  $\text{Hg}^p$ , respectively. This provincial inventory is thoroughly compared to three  
12 downscaled national inventories (NJU, THU and BNU) and two global ones  
13 (AMAP/UNEP and EDGARv4.tox2). Attributed to varied methods and data sources,  
14 clear information gaps exist in multi-scale inventories, leading to differences in the  
15 emission levels, speciation and spatial distributions of atmospheric Hg. The total  
16 emissions in the provincial inventory are 28%, 7%, 19%, 22%, and 70% larger than  
17 NJU, THU, BNU, AMAP/UNEP, and EDGARv4.tox2, respectively. For major sectors  
18 including power generation, cement, iron & steel and other coal combustion, the Hg  
19 contents ( $HgC$ ) in coals/raw materials, abatement rates of air pollution control devices  
20 (APCD) and activity levels are identified as the crucial parameters responsible for the  
21 differences in estimated emissions between inventories. Regarding speciated  
22 emissions, larger fraction of  $\text{Hg}^{2+}$  is found in the provincial inventory than national  
23 and global inventories, resulting mainly from the results by the most recent domestic  
24 studies in which enhanced  $\text{Hg}^{2+}$  were measured for cement and iron & steel plants.  
25 Inconsistent information on big power and industrial plants is the main source of  
26 differences in spatial distribution of emissions between the provincial and other  
27 inventories, particularly in southern and northwestern Jiangsu where intensive coal  
28 combustion and industry are located. Quantified with Monte-Carlo simulation,  
29 uncertainties of provincial inventory are smaller than those of NJU national inventory,  
30 resulting mainly from the more accurate activity data of individual plants and the  
31 reduced uncertainties of  $HgC$  in coals/raw materials.

删除的内容: sources

删除的内容: incorporated

删除的内容: released as

删除的内容: the downscaled results from

删除的内容: inventories

删除的内容: the largest, i.e.,

删除的内容: higher

删除的内容: of

删除的内容: Hg emissions

## 1 INTRODUCTION

33 Mercury (Hg), known as a global pollutant, has received increasing attention for  
34 its toxicity and long-range transport. Identified as the most significant release into the  
35 environment (Pirrone and Mason, 2009; AMAP and UNEP, 2013), atmospheric Hg is  
36 analytically defined as: gaseous elemental Hg (GEM, Hg<sup>0</sup>) that has longest lifetime  
37 and transport distance, and reactive gaseous mercury (RGM, Hg<sup>2+</sup>) and particle-bound  
38 mercury (PBM, Hg<sup>p</sup>) that are more affected by local sources. Improved estimates in  
39 emissions of speciated atmospheric Hg are believed to be essential for better  
40 understanding the global transport, chemical behaviors and mass balance of Hg.

41 Due mainly to the fast growth in economy and intensive use of fossil fuels, China  
42 has been indicated as the highest ranking nation in anthropogenic Hg emissions (Fu et  
43 al., 2012; Pacyna et al., 2010; Pirrone et al., 2010). Emissions of speciated  
44 atmospheric Hg of anthropogenic origin in China have been estimated at both global  
45 and national scales. For example, AMAP/UNEP (2013) and Muntean et al. (2014)  
46 developed global Hg inventories, which reported national emissions, for China for  
47 2010 and from 1970 to 2008, respectively. At national scale, Hg emissions have been  
48 estimated based on more detailed provincial information on energy consumption and  
49 industrial production. Zhang et al. (2015), Zhao et al. (2015a) and Tian et al. (2015)  
50 evaluated the inter-annual trends in emissions for 2000-2010, 2005-2012, and  
51 1949-2012, respectively, to explore the benefits of air pollution control policies,  
52 particularly for recent years.

53 There are considerable information gaps between inventories, attributed mainly  
54 to the data of different sources and levels of details. For coal-fired power plants (CPP),  
55 as an example, the global inventories by AMAP/UNEP (2013) and Muntean et al.  
56 (2014) obtained the national coal consumption from the International Energy Agency  
57 (IEA), and they acquired the information of control technologies from the “national  
58 comments” by selected experts and World Electric Power Plants database (WEPP),  
59 respectively. In the national inventories by Zhang et al. (2015) and Tian et al. (2015),  
60 coal consumption of CPP by province was derived from official energy statistics, and  
61 the penetrations of flue gas desulfurization (FGD) systems were assumed at provincial  
62 level. Zhao et al. (2015a) further analyzed the activity data and emission control levels  
63 plant by plant using a “unit-based” database of power sector. Although data of varied  
64 sources and levels of details result in discrepancies between inventories, those

删除的内容: with

删除的内容: -specific

删除的内容: reported

删除的内容: multi-scale

删除的内容: inventory

65 discrepancies and the underlying reasons have not been thoroughly analyzed in  
66 previous studies, leading to big uncertainty in Hg emission estimation.

67 Existing global and national inventories could hardly provide satisfying estimates  
68 in speciated Hg emissions or well capture the spatial distribution of emissions at  
69 regional/local scales, attributed mainly to relatively weak investigation on individual  
70 sources. When they are used in chemistry transport model (CTM), downscaled  
71 inventories at global/national scales would possibly bias the simulation at smaller  
72 scales. Improvement in emission estimation at local scale, particularly for the large  
73 point sources is thus crucial for better understanding the atmospheric processes of Hg  
74 (Lin et al., 2010; Wang et al., 2014; Zhu et al., 2015). While local information based  
75 on sufficient surveys is proven to have advantages in improving the emission  
76 estimates for given pollutants like NO<sub>x</sub> and PM<sub>10</sub> (Zhao et al., 2015b; Timmermans et  
77 al., 2013), there are currently very few studies ~~on Hg emissions~~ at regional/local  
78 scales in China, and the differences of multi-scale inventories remain unclear.

删除的内容: focusing

79 In this work, therefore, we select Jiangsu, one of the most developed provinces  
80 with serious air pollution in China, as study area. Firstly, we develop a high-resolution  
81 Hg emission inventory of anthropogenic origin for 2010, based on comprehensive  
82 review of field measurements and detailed information on emission sources. That  
83 provincial inventory is then compared to selected global and national inventories with  
84 a thorough analysis on data and methods. ~~Discrepancies in emission levels, speciation,~~  
85 and spatial distributions are evaluated and the underlying sources of the discrepancies  
86 are figured out. Finally, the uncertainty of the provincial emission inventory is  
87 quantified and the key parameters contributing to the uncertainty are identified. The  
88 results provide an insight on the effects of varied approaches and data on development  
89 of Hg emission inventory, and indicate the limitations of current studies and the  
90 orientations for further improvement on emission estimation at regional/local scales.

删除的内容: of multi-scale inventories

91

92

## 2 DATA AND METHODS

### 93 2.1 Data sources of multi-scale inventories

94 As shown in Figure S1 in the supplement, Jiangsu province (30°45' N-35°20' N,  
95 116°18' E-121°57' E) is located in Yangtze River Delta in eastern China and covers 13  
96 cities. The Hg emissions of Jiangsu are obtained from two approaches: downscaled  
97 from global/national inventories, and estimated using a bottom-up method with

98 information of local sources incorporated.

99 In global/national inventories, Hg emissions were first calculated by sector based  
100 on activity data and emission factors that were obtained or assumed at global, national  
101 or provincial level, and were then downscaled to regional domain with finer spatial  
102 resolution. Various methods and data were adopted in multi-scale inventories to  
103 estimate Hg emissions for different sectors, as summarized briefly in Table S1 in the  
104 supplement. Three national inventories were developed by Nanjing University (NJU,  
105 Zhao et al., 2015a), Beijing Normal University (BNU, Tian et al., 2015), and Tsinghua  
106 University (THU, Zhang et al., 2015), with major activity data at provincial level  
107 obtained from Chinese national official statistics. Compared to NJU and BNU  
108 inventories that applied deterministic parameters relevant to emission factors, THU  
109 developed a model with probabilistic technology-based emission factors to calculate  
110 the emissions. Based on international activity statistics at national level, two global  
111 inventories for 2010 were developed by the joint expert group of Arctic Monitoring  
112 and Assessment Programme and United Nations Environment Programme  
113 (AMAP/UNEP, 2013), and Emission Database for Global Atmospheric Research  
114 (EDGARv4.tox2, unpublished). AMAP/UNEP inventory developed a new system for  
115 estimating emissions from main sectors based on a mass-balance approach with data  
116 on unabated emission factors and emission reduction technology employed in  
117 different countries. EDGARv4.tox2 inventory calculated the emissions for all the  
118 countries by primarily applying emission factors from EEA (2009) and USEPA (2012),  
119 combined with regional technology-specific information of emission abatement  
120 measures.

121

## 122 2.2 Development of the provincial inventory

123 In contrast to the downscaling approach, the emissions are calculated plant by  
124 plant based on information of individual sources and then aggregated to provincial  
125 level in a bottom-up method. We mention the inventory as bottom-up or provincial  
126 inventory hereinafter. Information for individual emission sources are thoroughly  
127 obtained from Pollution Source Census (PSC, internal data from Environmental  
128 Protection Agency of Jiangsu Province). PSC was conducted by local environmental  
129 protection agencies, in which the data for individual sources were collected and  
130 compiled through on-site investigation, including manufacturing technology,  
131 production level, energy consumption, fuel quality, and emission control device.

删除的内容: a bottom-up method is further applied, in which

删除的内容: first

删除的内容: at

删除的内容: collected

删除的内容: , including combustion technology, fuel quality and air pollutant control devices.

132 Differences in total energy consumption and industrial production levels exist  
133 between the PSC data and the energy/economic statistics. For example, the coal  
134 consumption by power plants in PSC was 6% larger than the provincial statistics for  
135 Jiangsu 2010. Compared to the energy and economic statistics that were commonly  
136 used in global/national inventories, we believe the plant-by-plant PSC data could  
137 provide more detailed and accurate information on specific emitters, particularly for  
138 power and industrial plants.

139 According to the availability of data, anthropogenic sources are classified into  
140 three main categories. Category 1 includes coal-fired power plants (CPP), iron & steel  
141 plants (ISP), cement production (CEM) and other industrial coal combustion (OIB).  
142 Note that the emissions from coal combustion in cement production are not included  
143 in CEM but in OIB, following most other inventories included in this paper for easier  
144 comparison. The information on geographic location, activity levels (consumption of  
145 energy or raw materials) and penetration of air pollution control devices (APCDs) is  
146 compiled plant by plant from PSC, with an exception that the technology employed in  
147 CEM are obtained from CCA (2011). Category 2 includes nonferrous metal smelting  
148 (NMS), aluminum production (AP), municipal solid waste incineration (MSWI) and  
149 intentional use sector (IUS: thermometer, fluorescent lamp, battery and polyvinyl  
150 chloride polymer production). Geographic location information for those sources is  
151 obtained from PSC, while other activity data come from official statistics at provincial  
152 level. Category 3 includes emission sources that are not contained in Pollution Source  
153 Census: residential & commercial coal combustion (RCC), oil & gas combustion  
154 (O&G), biofuel use/biomass open burning (BIO), rural solid waste incineration  
155 (RSWI) and human cremation (HC). They are defined as area sources, and the data  
156 sources for them are discussed later in this section.

删除的内容: involved

删除的内容: work

删除的内容: Pollution Source Census

删除的内容: Pollution Source Census

157 In general, annual emissions of total and speciated Hg are calculated using Eq. (1)  
158 and (2), respectively:

$$E = \sum_n AL_n \times EF_n \quad (1)$$

$$E_s = \sum_n AL_n \times EF_n \times F_{n,s} \quad (2)$$

159 where  $E$  is the Hg emission;  $AL$  is the activity levels (fuel consumption or industrial  
160 production);  $EF$  is the combined emission factor (emissions per unit of activity level);  
161  $F$  is the mass fraction of given Hg speciation;  $n$  and  $s$  represent emission source type

162 and Hg speciation ( $\text{Hg}^0$ ,  $\text{Hg}^{2+}$  or  $\text{Hg}^p$ ).

163 For CPP/OIB and CEM, Eq. (1) can be revised to Eq. (3) and (4) respectively,  
164 with detailed fuel and technology information of individual sources incorporated:

$$E_{CPP/OIB} = \sum_t \sum_i \sum_k AL_i \times HgC_k \times RR_t \times (1 - RE_t) \quad (3)$$

$$E_{CEM} = \sum_t \sum_i (AL_{Limestone} \times HgC_{Limestone} + AL_{Other,i} \times HgC_{Other}) \times (1 - RE_t) \quad (4)$$

165 where  $HgC$  is the Hg content of coal consumed in Jiangsu, calculated based on  
166 measured Hg contents of coal mines across the country and an inter-provincial flow  
167 model of coal transport (Zhang et al., 2015);  $HgC_{Limestone}$  and  $HgC_{Other}$  represent Hg  
168 contents of limestone and other raw materials (e.g. malmstone and iron powder) in  
169 cement production, respectively;  $RR$  is the Hg release ratios from combustors;  $RE$  is  
170 Hg removal efficiency of APCDs;  $AL_{Limestone}$  and  $AL_{Other}$  represent the consumption of  
171 limestone and other raw materials in CEM, respectively;  $i$  and  $k$  represent individual  
172 point source and coal type, respectively;  $t$  represent APCD type including wet  
173 scrubber (WET), cyclone (CYC), fabric filter (FF), electrostatic precipitator (ESP),  
174 FGD and selective catalyst reduction (SCR) systems for CPP, and dry-process  
175 precalciner technology with dust recycling (DPT+DR), shaft kiln technology (SKT)  
176 and rotary kiln technology (RKT) with ESP or FF for CEM. Note the  $AL$  for  
177 individual CEM plant is calculated based on the clinker and cement production when  
178 the information on limestone or other raw materials is missing in PSC.

179 For ISP, Eq. (1) could be revised to Eq. (5):

$$E_{ISP} = \sum_i (AL_{steel,i} + AL_{iron,i} \times R) \times EF_{steel} \quad (5)$$

180 where  $AL_{steel}$  and  $AL_{iron}$  represent crude steel and pig iron production in ISP,  
181 respectively;  $R$  is the liquid steel to hot metal ratio provided by BREF (2012),  
182 converting the production of pig iron to crude steel equivalent;  $EF_{steel}$  is the Hg  
183 emission factor applied to steel making, obtained from recent domestic tests by Wang  
184 et al. (2016).

185 Activity data for NMS, AP, MSWI, RCC and O&G are derived from national  
186 statistics (NMIA, 2011; NSB, 2011a; 2011b), while Hg consumption in IUS are  
187 estimated based on the internal industry reports that provide national market and  
188 economy information collected at <http://www.askci.com/>. Activity data for MSWI,  
189 RSWI and BIO are taken following Zhao et al. (2015a). Other information including

删除的内容: The biofuel use is obtained from the investigation by Ministry of Agriculture (C. Chen et al., 2013). The biomass combusted in open fields is originally calculated as a product of grain production, waste-to-grain ratio, and the percentage of residual material burned in the field, as described in Zhao et al. (2011, 2012). The rural municipal waste burned are calculated as a product of rural population, the average waste per capita, and the ratios of waste that is burned (Yao et al., 2009).

190 control efficiencies of APCDs, speciation profiles and emission factors inherited from  
191 previous studies is summarized in Table S2-S4 in the supplement.

192 Regarding the spatial pattern of emissions, the study domain is divided into 4212  
193 grid cells with a resolution at  $0.05^\circ \times 0.05^\circ$ . For Categories 1 and 2, emissions are  
194 directly allocated into corresponding grid cells according to the locations of individual  
195 sources. As considerable errors of plant locations were unexpectedly found in PSC,  
196 the geographic location for point sources with emissions more than 15 kg have been  
197 corrected by Google Map. As a result, totally 900 plants are relocated, accounting for  
198 14% of all the point sources. For Category 3, emissions are allocated according to the  
199 population density in urban areas (RCC) and that in rural areas (BIO and RSWI).

200

### 201 | 2.3 Sensitivity and uncertainty analysis of emissions

202 For better understanding the sources of discrepancies between inventories, a  
203 comprehensive sensitivity analysis is conducted to quantify the differences between  
204 selected parameters used in multi-scale inventories and the subsequent changes in  
205 emission estimation for Category 1 sources. The relatively change ( $RC$ ) of given  
206 parameter ( $j$ ) in global/national inventories compared to those in the provincial  
207 bottom-up inventory, and the changes in emissions for selected source ( $n$ ) when the  
208 value of parameter  $j$  in the bottom-up inventory is replaced by that in global/national  
209 inventories ( $E_{diff,n}$ ), can be calculated using Eqs. (6) and (7), respectively:

$$RC_j = (VO_j - VB_j) / VB_j \quad (6)$$

$$E_{diff,n} = EO_n - EB_n \quad (7)$$

210 where  $VB$  is the value of parameters in bottom-up inventory;  $VO$  is the value of  
211 parameters in other national/global inventories;  $EB$  is Hg emissions for given sector in  
212 bottom-up inventory;  $EO$  is Hg emissions for given sector when the values of  
213 parameters in bottom-up inventory are replaced by those in other global/national  
214 inventories;  $j$  and  $n$  represent given parameter and source type, respectively.

215 In particular, a new parameter, total abatement rate ( $TA$ ), is defined for the  
216 sensitivity analysis, combining the effect of the penetrations of APCDs and their  
217 removal efficiencies on emission abatement:

$$TA = \sum_t AR_t \times RE_t \quad (8)$$

218 where  $t$  represents APCD type;  $AR$  and  $RE$  are the application rate and Hg removal

删除的内容: Hg

删除的内容: given

带格式的: 字体: 倾斜



219 efficiency, with detailed information provided in Table S5 in the supplement.

220 The uncertainties of speciated Hg emissions at provincial level are quantified  
221 using a Monte-Carlo framework (Zhao et al., 2011). Given the relatively accurate data  
222 reported in PSC, the probability distributions of activity levels for individual plants of  
223 CPP, OIB, ISP and CEM are defined as normal distributions with the relative standard  
224 deviations (RSD) set at 10%, 20%, 20% and 20% respectively. As summarized in  
225 Table S6 and Table S7 in the supplement, a database for Hg emission factors/related  
226 parameters by sector and speciation are established for China, with the uncertainties  
227 analyzed and indicated by probability distribution function (PDF). The PDFs of Hg  
228 contents in coal mines by province are obtained from Zhang et al. (2015). For Hg  
229 content in limestone ( $HgC_{Limestone}$ ), a lognormal distribution is generated with  
230 bootstrap simulation based on 17 field tests by Yang (2014), as shown in Figure S2 in  
231 the supplement. For the rest parameters, a comprehensive analysis of uncertainties  
232 were conducted, incorporating the data from available field measurements, as  
233 described in Zhao et al. (2015a). Ten thousand simulations are performed to estimate  
234 the uncertainties of emissions, and the parameters that are most significant in  
235 determination of the uncertainties are identified by source type according to the rank  
236 of their contributions to variance.

删除的内容: for main sources

删除的内容: uncertainty

删除的内容: presented

删除的内容: with the results

删除的内容: of

删除的内容: available fully incorporated

237

## 238 3 RESULTS AND DISCUSSIONS

### 239 3.1 Emission estimation and comparison by sector

#### 240 3.1.1 The total Hg emissions from multi-scale inventories

241 Table 1 provides the Hg emissions by sector and species for Jiangsu 2010  
242 estimated from the bottom-up approach. The provincial total Hg emissions of  
243 anthropogenic origin are calculated at 39 105 kg, of which 51% released as  $Hg^0$ , 47%  
244 as  $Hg^{2+}$ , and 2% as  $Hg^P$ . In general, Categories 1, 2 and 3 account for 90%, 4% and  
245 6% of the total emissions, respectively. CPP and CEM are the biggest  
246 contributors to the total Hg ( $Hg^T$ ) emissions. For  $Hg^0$ ,  $Hg^{2+}$ , and  $Hg^P$ , the sectors with  
247 the largest emissions are CPP, CEM, and OIB respectively.

248 To better understand the discrepancies and their sources between various studies,  
249 the emissions from multi-scale inventories are summarized in Table 1 for comparison.  
250 Among all the inventories, the total emissions in the provincial inventory are the

删除的内容: also

251 largest, i.e., 28%, 7%, 19%, 22%, and 70% higher than NJU, THU, BNU,  
252 AMAP/UNEP, and EDGARv4.tox2, respectively. The elevated Hg emissions  
253 compared to previous studies could be supported by modeling and observation work  
254 to some extent. Based on the chemistry transport modeling using GEOS-Chem (Wang  
255 et al., 2014), or correlation slopes with certain tracers (CO, CO<sub>2</sub> and CH<sub>4</sub>) from  
256 ground observation (Fu et al., 2015), underestimation was suggested for the regional  
257 Hg emissions of anthropogenic origin in China.

258 Direct comparison between inventories is unavailable for every sector, as the  
259 definition of source categories is not fully consistent with each other. Therefore,  
260 necessary assumption and modification are made on source classification for global  
261 inventories. In Table 1, CPP, OIB and RCC for EDGARv4.tox2 actually represent the  
262 emissions for all the fossil fuel types, and they are 1316, 5342 lower and 986 kg  
263 higher than our estimation from coal combustion, respectively. For AMAP/UNEP, the  
264 emissions from regrouped stationary combustion (industrial sources excluded),  
265 industry, and intentional use and product waste associated sources (see Table 1 for the  
266 detailed definition) are respectively 3382, 2032 higher and 3118 kg lower than our  
267 estimation with bottom-up method. Figure 1 shows the ratios of the estimated Hg  
268 emissions in national/global inventories to those in the provincial inventory by source.  
269 The CPP emissions are relatively close to each other, but larger differences exist in  
270 some other sources. The estimates for CEM and ISP in provincial inventory are much  
271 higher than NJU, BNU and EDGARv4.tox2 inventories, while those for NMS are  
272 extremely smaller. The reasons for those differences are analyzed in details in  
273 Sections 3.1.2-3.1.4.

### 274 3.1.2 Sensitivity analysis for **power plants and industrial boilers**

275 Figure 2 (a) and (b) represents the relative changes in given parameters between  
276 the provincial and other inventories, and the subsequent differences in Hg emissions  
277 for Category 1 sources, using Eqs. (6) and (7), respectively. For CPP, the differences  
278 between provincial and national/global inventories are mainly determined by *AL*, *HgC*,  
279 *TA*, and *IEF*, as indicated by the calculation methods summarized in Table S1.  
280 (Instead of analyzing *HgC* and *RR* separately, integrated input emission factors (*IEF*)  
281 were applied in AMAP/UNEP and EDGARv4.tox2.) For activity level (*AL*), the  
282 coal consumption data are collected and compiled plant by plant in the provincial  
283 inventory, while they were obtained from Chinese official statistics (NSB, 2011b) in

删除的内容: of emissions

删除的内容: discussed and

删除的内容: and

删除的内容: 3

删除的内容: Category 1 sources

284 national inventories. As a result, the coal consumptions in NJU and THU inventories  
285 are 17% and 6% smaller than our provincial inventory, resulting in 1968 and 760 kg  
286 reduction in Hg emission estimate, respectively.

287 In national and provincial inventories, as mentioned in Section 2, the Hg contents  
288 in the raw coal ( $HgC_{raw}$ ) consumed by province are estimated using an  
289 inter-provincial flow matrix for coal transport based on the results of field  
290 measurements on Hg contents for given coal mines (Tian et al., 2010; Tian et al., 2014;  
291 Zhang et al., 2012). The  $HgC_{raw}$  for Jiangsu in THU and our provincial inventory  
292 come from Zhang et al. (2012), who merged the results of two comprehensive  
293 measurement studies on  $HgC_{raw}$  for coal mines across China after 2000, by  
294 themselves and USGS (2004), and the average value is calculated at 0.2 g/t-coal. NJU  
295 inventory adopted the  $HgC_{raw}$  of 0.169 g/t-coal from Tian et al. (2010), while BNU  
296 inventory determined  $HgC_{raw}$  at 0.25 g/t-coal with a bootstrap simulation based on a  
297 thorough investigation on published data (Tian et al., 2014).  $HgC_{raw}$  in NJU and BNU  
298 inventories are 15% smaller and 25% higher than that in provincial inventory, leading  
299 to differences of 1746 and 2816 kg in Hg emissions, respectively. Given the large  
300 differences in  $HgC_{raw}$  between countries, global inventories applied national specific  
301 IEF based on the domestic tests (UNEP, 2011b; Wang et al., 2010). The IEFs for  
302 China applied in AMAP/UNEP and EDGARv4.tox2, without considering the  
303 regional differences in  $HgC_{raw}$ , are 26% and 28% lower than that in provincial  
304 inventory (recalculated with  $HgC_{raw}$  and  $RR$ ). As regional  $HgC_{raw}$  differs a lot from  
305 the national average and could be largely influenced by the data selected, big  
306 discrepancy might exist when national value is applied in regional inventory, and  
307 more regional-specific measurements are suggested for reducing the uncertainty.

删除的内容: constraining

308 Total abatement rate ( $TA$ ) of APCDs installed for CPP is calculated at 57% in the  
309 provincial inventory, 6.7 % and 8.2% smaller than that in THU and AMAP/UNEP  
310 inventories, respectively, and 12% larger than that in NJU inventory. The differences  
311 result mainly from the varied removal efficiencies ( $RE$ ) and application ratios ( $AR$ ), as  
312 shown in Table S5. For  $RE$ , local tests on FF, ESP+FGD and SCR+ESP+FGD were  
313 conducted by JSEMC (2013) and Xie and Yi (2014), and the results (provided in  
314 Table S2) are applied in the provincial inventory. From investigation on individual  
315 plants, the  $AR$  of FGD systems with relatively large benefits on Hg removal was  
316 underestimated in NJU and overestimated in THU inventory. In the AMAP/UNEP  
317 inventory, relevant parameters were obtained from national comment, and elevated  $TA$

318 was estimated due to the larger *AR* of FF and FGD and the higher *RE* of FGD+ESP  
319 compared to those obtained from detailed source investigation in the provincial  
320 inventory.

321 For OIB, the comparison of *HgC* is similar to that for CPP. *AL* from PSC in  
322 provincial inventory is very close to that in THU inventory obtained from NSB  
323 (2011b), while *AL* in NJU inventory was much lower as the coal consumption of  
324 CEM and ISP were excluded. The *RR* from industrial boilers in this work is estimated  
325 at 82% based on domestic measurements (Wang et al., 2000; Tang et al., 2004), much  
326 lower than the result in THU inventory measured by Zhang et al. (2012), i.e., 95% for  
327 stoker fired boiler. Given the limited samples in both inventories, large uncertainty  
328 exists in *RR* of industrial boilers. Compared to the provincial inventory, *ARs* of ESP  
329 and FGD were clearly underestimated in NJU and THU inventories (Table S5), hence  
330 the *TA* in NJU was calculated 23% smaller than that in provincial inventory, leading to  
331 a 747 kg increase in Hg emission estimate. In THU inventory, however, the much  
332 higher *RE* of WET reduced the difference between national and provincial inventories,  
333 and *TA* in THU inventory was only 2% smaller than the provincial one.

### 334 **3.1.3 Sensitivity analysis for cement and iron & steel industries**

335 ~~For CEM, both the provincial and THU inventories adopted the data from Yang~~  
336 (2014), who measured provincial Hg contents in raw materials (limestone and other  
337 raw materials) and Hg removal efficiency of DPT+DR in China. For *AL*, the  
338 limestone consumption were calculated based on the clinker and cement production of  
339 individual plants in the provincial inventory, while THU relied on cement production  
340 at provincial level, leading to 13% smaller in *AL* and 1019 kg reduction in Hg  
341 emission estimate. In addition, consumption of other raw materials for CEM were  
342 ignored in THU inventory, leading to 1223 kg smaller in emission estimate compared  
343 to the provincial inventory. According to on-site survey by Yang (2014), fly ash is  
344 100% reused in DPT+DR, thus the technology minimizes the Hg removal by dust  
345 collectors (ESP or FF). The *AR* of DPT+DR in THU was estimated at 82% at national  
346 average level, while it reaches 89% in Jiangsu based on detailed provincial statistics  
347 (CCA, 2011). Hence the *TA* employed in THU is 25% larger than that in provincial  
348 inventory, resulting in 259 kg underestimation in Hg emissions. NJU and  
349 AMAP/UNEP inventories failed to characterize the poor control of Hg from DPT+DR.  
350 *EFs* applied in NJU came from early domestic measurements on rotary and shaft kiln

删除的内容:

351 (Li, 2011; Zhang, 2007), ignoring the recent penetration of DPT+DR. In  
352 AMAP/UNEP inventory, an effective Hg capture of 40% was generally assumed for  
353 China's cement plants taking only the use of ESP and FF into account. The *TA* was  
354 estimated 215% larger than that in the provincial inventory, resulting in 2253 kg  
355 reduction in Hg emission estimate. EDGAR applied uniform emission factor (UEF) of  
356 0.065g/t-clinker from EEA (2009), 32% lower than the average *EF* in the provincial  
357 inventory. BNU developed S-shaped curves to estimate the time-varying dynamic  
358 emission factors for non-coal combustion sector, based on the assumption of a  
359 gradually declining trend in *EFs* along with increased controls of APCDs. As  
360 mentioned above, however, the trend was not suitable for CEM due to the penetration  
361 of DPT+DR. Thus UEF of 0.02 g/t-cement estimated in BNU might result in  
362 underestimation in Hg emissions, e.g., 7261 kg smaller than our provincial inventory.

删除的内容: t

363 For ISP, difficulty exists in emission estimation due to various Hg input sources  
364 and complex production processes, and there is no consistent method in multi-scale  
365 inventories so far. It was found that raw material production (limestone and dolomite),  
366 coking, sintering and pig iron smelting with blast furnace account for most Hg  
367 emissions in typical ISP in China (Wang et al., 2016). In our study, 11 factories  
368 containing those processes are collected in PSC, and the emissions factors of 0.043  
369 and 0.068 g/t-crude steel from Wang et al. (2016) are applied to plants with and  
370 without raw material production, respectively. In other inventories, very few results  
371 from domestic measurements were applied for Hg emission estimation for ISP in  
372 China. NJU took only coal combustion into account, and thus underestimated the  
373 emissions for the sector by neglecting the Hg input along with iron ore, limestone and  
374 other raw materials. THU applied an emission factor of 0.04 g/t from Pacyna et al.  
375 (2010) for crude steel production. Besides difference in emission factors, THU did not  
376 count the pig iron production in *AL* estimation, thus *AL* in THU inventory is 29%  
377 lower than that in the provincial inventory, resulting in 1615 kg reduction in Hg  
378 emission estimate. Average *EF* in AMAP/UNEP was estimated at 0.039 g/t-pig iron  
379 by combining the input factor (0.05g/t-pig iron) calculated with a mass balance  
380 method (UNEP, 2011a; BREF, 2012), and the removal effects of APCDs. For  
381 comparison, *EF* used in our provincial inventory was recalculated at 0.064 g/t-pig iron  
382 based on the hot metal charging ratio (*R* in Eq. (5); BREF, 2012). Lower *EF* in  
383 AMAP/UNEP can partly be attributed to the overestimated *AR* of APCDs in ISP  
384 without considering the gradual penetration of dust recycling as in CEM.

删除的内容: inventory

删除的内容: inventory

删除的内容: the

385 In general, the detailed activity and technology information including  
386 manufacturing procedures and APCDs were investigated for individual plants in our  
387 provincial inventory to improve the emission estimation, in contrast to previous  
388 inventories that applied simplified or regional-average data. However, some crucial  
389 parameters, e.g., Hg contents in coal and limestone, and Hg removal efficiencies of  
390 APCDs, are still unavailable at plant level due to lack of measurements. Such  
391 limitation indicates the necessity of more efforts on plant-specific emission factors,  
392 and also motivates the uncertainty analysis for the provincial inventory, as presented  
393 in Section 3.4.

删除的内容: thus

### 394 **3.1.4 Comparisons of emissions for Categories 2 and 3**

删除的内容: 3

395 For Categories 2 and 3, differences also exist in *EF* and *AL* between inventories.  
396 For example, an emission factor of 0.22 g/t-waste combusted for MSWI based on  
397 domestic tests (L. Chen et al., 2013; Hu et al., 2012) is applied in the provincial  
398 inventory, while THU applied 0.5 g/t from UNEP (2005), resulting in a difference of  
399 1024 kg in emission estimate. For primary Cu production, the provincial inventory  
400 applied the emission factor of 0.4g/t-Cu from Wu et al. (2012), who incorporated the  
401 results of available field measurements and the penetrations of different smelting  
402 processes in China. BNU, however, applied a much higher emission factor at 8.9  
403 g/t-Cu estimated by using an S-shaped curve based on international results (Habashi,  
404 1978; Nriagu, 1979; Pacyna, 1984; Pacyna and Pacyna, 2001; Streets et al., 2011;  
405 EEA, 2013). In NJU inventory, the emissions from NMS and IUS were estimated  
406 much higher than the provincial inventory, attributed largely to the different sources  
407 of activity data. For NMS, activity levels in NJU and provincial inventories were  
408 obtained from NSB (2011c) and NMIA (2011), respectively. While NMIA (2011)  
409 provides the information on the production of primary nonferrous metal (the major  
410 source of Hg emissions for NMS), the secondary production were included in NSB  
411 (2011c), leading to possible overestimate in *AL* and thereby Hg emissions. For IUS,  
412 provincial Hg consumption was allocated from the national total use weighted by  
413 GDP in NJU inventory, while the data are directly derived for Jiangsu from internal  
414 industrial report in the provincial inventory. In the global inventories, moreover, all  
415 the emissions for Categories 2 and 3 in Jiangsu were downscaled from national  
416 estimations attributed to lack of provincial information, and big bias could be  
417 expected. For example, the large discrepancy for intentional use and product waste

删除的内容: inventory

删除的内容: inventory

删除的内容: study

删除的内容: generated

418 associated sources between downscaled global and provincial inventories is likely  
419 attributed to the overestimation in emissions from artisanal and small-scale gold  
420 mining (ASGM) by global inventory (not included in Table 1 as no ASGM was found  
421 by local source investigation).

422

### 423 **3.2 Hg speciation analysis of multi-scale inventories**

424 Besides the total emissions, Hg speciation has a significant impact on the  
425 distance of Hg transport and chemical behaviors. Table 2 summarizes the mass  
426 fractions of Hg species in emissions by sector for multi-scale inventories.

427 In general, as shown in Table 2, reduced  $\text{Hg}^0$  but enhanced  $\text{Hg}^{2+}$  is estimated as  
428 the spatial scale gets smaller. This can be mainly explained by the use of domestic  
429 measurement results on Hg speciation for CEM, ISP and MSWI in the provincial  
430 inventory. For CEM, the  $\text{Hg}^{2+}$  mass fraction for the dominating DPT+DR technology  
431 tends to reach 75% based on available measurements (Yang, 2014), leading to a much  
432 larger fraction of  $\text{Hg}^{2+}$  emissions in the provincial inventory. In contrast, speciated Hg  
433 emissions were calculated using the same speciation profiles as those for coal  
434 combustion in NJU inventory or the uniform profile ignoring the effects of APCDs in  
435 AMAP/UNEP inventory. For ISP, heterogeneous Hg oxidation can be enhanced by the  
436 high concentration of dust and existence of  $\text{Fe}_2\text{O}_3$  in the flue gas during sintering  
437 process, leading to large  $\text{Hg}^{2+}$  fraction for the sector reaching 66% (Wang et al., 2016).  
438 For MSWI, results of domestic measurements (L. Chen et al., 2013; Hu et al., 2012)  
439 were applied in the provincial and NJU inventories, elevating the  $\text{Hg}^{2+}$  fraction  
440 compared to THU and AMAP/UNEP inventories that applied a global uniform  
441 speciation profile without consideration of regional difference. It should be noted,  
442 however, that uncertainty exists in the estimation of speciated emissions at small  
443 spatial scale, attributed mainly to the limited samples in domestic measurements on  
444 CEM and ISP.

445 As mentioned above, the “universal” profiles were applied for many sectors in  
446 AMAP/UNEP inventory, ignoring the effects of various types of APCDs on Hg  
447 speciation, particularly for coal combustion. However, the fate of Hg released to  
448 atmosphere can primarily be affected by the removal mechanisms of APCDs. As  
449 shown in Table 3, for example,  $\text{Hg}^0$  mass fractions for ESP+FGD and FF+FGD tend  
450 to be high reaching 83% and 78%, respectively, attributed to the relatively strong  
451 removal effects of APCDs on  $\text{Hg}^{2+}$  and  $\text{Hg}^p$ . Once SCR is applied, an increase of  $\text{Hg}^{2+}$

452 fraction can be observed, as the catalyst in SCR system can accelerate the conversion  
453 of  $\text{Hg}^0$  to  $\text{Hg}^{2+}$  (Wang et al., 2010). In addition,  $\text{Hg}^0$  can also be oxidized to  $\text{Hg}^{2+}$  in FF  
454 attributed to specific chemical composition in flue gas (chlorine, for example) and to  
455 high temperature (Wang et al., 2008; He et al., 2012). In contrast to global inventories,  
456 therefore, national and provincial inventories take the effects of different APCDs into  
457 account. Summarized in Table 3, considerable differences exist in the speciation  
458 profiles for typical APCDs between national and provincial inventories, attributed  
459 mainly to the various data used from domestic field measurements. Excluding the  
460 measurement results on WET (Zhang et al., 2012), NJU assumed same species profile  
461 for WET, and CYC, and thereby largely underestimated the mass fraction of  $\text{Hg}^0$  for  
462 OIB where WET is widely applied. Besides, the penetrations of APCDs are also  
463 crucial in determination of speciated Hg emissions. As indicated in Table 3, with  
464 similar speciation profiles for FGD applied between multi-scale inventories, the  
465 difference in Hg speciation is relatively small for CPP between inventories, given the  
466 relatively accurate and transparent information on FGD penetration in CPP. For OIB,  
467 however, the difference in Hg speciation is significantly elevated, as large diversity in  
468 APCDs penetration is found between multi-scale inventories, as shown in Table S5.  
469 With the penetration of FF and ESP highly underestimated, for example, THU  
470 provided a lower estimation in  $\text{Hg}^{2+}$  fraction compared to other inventories.

删除的内容: for example,

删除的内容: inventory

删除的内容: the

删除的内容: ro

删除的内容: m

删除的内容: to be the same as

删除的内容: used in all the inventories

### 472 3.3 Comparisons of spatial patterns of emissions between multi-scale inventories

473 Figure 3 presents the spatial distributions of total and speciated Hg emissions in  
474 Jiangsu province at  $0.05^\circ \times 0.05^\circ$ . Similar patterns are found between species.  
475 Relatively high emissions are distributed over northwestern and southern Jiangsu,  
476 resulting from intensive coal combustion, and cement and iron & steel production, as  
477 indicated in Figure S1 in the supplement. As an important energy base, Xuzhou in  
478 northwestern Jiangsu contains a large number of coal combustion sources, while great  
479 energy demand exists in southern Jiangsu attributed to developed economy and  
480 intensive industry. For cement production, as an example, the clinker manufacture  
481 plants that dominate the Hg emissions compared to the subsequent mixing stage  
482 (UNEP, 2011a), are mainly located in southern Jiangsu, depending on the distribution  
483 of limestone resources.

删除的内容: highly

删除的内容: The gross industrial production of the five cities in southern Jiangsu (Nanjing, Zhenjiang, Suzhou, Wuxi and Changzhou) in 2010 accounted for 64% of the total amount in the province.

484 In order to compare the spatial distribution of provincial inventory to that of NJU,  
485 THU, AMAP/UNEP and EDGARv4.tox2 inventories, we upscale the gridded



486 provincial emissions from  $0.05^{\circ} \times 0.05^{\circ}$  to the resolutions of  $0.125^{\circ} \times 0.125^{\circ}$ ,  $36 \times 36 \text{ km}$ ,  
487  $0.5^{\circ} \times 0.5^{\circ}$  and  $0.1^{\circ} \times 0.1^{\circ}$  respectively. Differences in gridded  $\text{Hg}^{\text{T}}$  emissions for  
488 Jiangsu between the upscaled provincial inventory and other multi-scale inventories  
489 are presented in Figure 4. Although selected sources were identified as point sources  
490 in global/national inventories, e.g., CEM in NJU and THU, ISP in EDGARv4.tox2,  
491 and CPP in all the inventories, the emission fraction of point sources (Categories 1  
492 and 2) is significantly elevated to 92% in the provincial inventory. In particular, the  
493 emissions from point sources of which the geographic information were corrected  
494 account for 78% of total emissions in the province.

495 As illustrated in Figure 4, differences in gridded emissions between provincial  
496 and other inventories NJU, THU, AMAP/UNEP and EDGARv4.tox2 are respectively  
497 in the ranges of  $-760 \sim +4135 \text{ kg}$ ,  $-1429 \sim +3217 \text{ kg}$ ,  $-1424 \sim +3043 \text{ kg}$  and  $-1078 \sim +3895$   
498  $\text{kg}$ . Grids with differences more than  $400 \text{ kg/yr}$  are commonly distributed in southern  
499 and northwestern Jiangsu, and coincide well with the locations of point sources with  
500 relatively large emissions in the provincial inventory. It can be indicated that  
501 differences in spatial patterns of Hg emissions come mainly from the inconsistent  
502 information of big point sources between the provincial inventory and national/global  
503 inventories. For CPP, AMAP/UNEP obtained information of identified facilities from  
504 Wikipedia ([http://en.wikipedia.org/wiki/List\\_of\\_power\\_stations\\_in\\_Asia](http://en.wikipedia.org/wiki/List_of_power_stations_in_Asia)), and failed  
505 to include a number of coal-fired power plants built in recent years (Steenhuisen et al.,  
506 2015). For EDGARv4.tox2, proxy data (e.g., electricity production) from Carbon  
507 Monitoring Action (CARMA, <http://carma.org/blog/carma-notes-future-data/>) are  
508 used to allocate Hg emissions. Although CARMA incorporates all the major  
509 disclosure databases, uncertainties exist in certain individual plants attributed to lack  
510 of information on geographical locations and control technologies. Moreover, as the  
511 most updated information in CARMA was collected in 2009, EDGAR had to predict  
512 the emissions of CPP for 2010, and could not fully track the actual changes in the  
513 sector, e.g., operation of new-built units, or shutting down the small ones. Similarly,  
514 NJU and THU obtained the information of power units from a relatively old database  
515 (Zhao et al., 2008), and made further assumptions on activities and penetrations of  
516 APCDs to update the emissions of individual plants. As a result, in general, larger  
517 emissions are found in the provincial inventory than other inventories in southern  
518 Jiangsu where big power plants are located, particularly in Nanjing and northern  
519 Suzhou. As detailed information at plant level is unavailable for each inventory, we

删除的内容: that are estimated to have

删除的内容: thus

删除的内容: still

删除的内容: thus

520 speculate the discrepancy resulted mainly from the underestimation (or missing) in  
521 coal consumption in previous electric power generation databases that other  
522 inventories relied on, and from the use of regional/national-average information on  
523 APCD penetration by certain inventories (e.g., THU and AMAP/UNEP). The  
524 comparison in northwestern Jiangsu is less conclusive: the emissions in the areas with  
525 big power plants were estimated lower in provincial inventory than AMAP/UNEP  
526 (Figure 4(c)). Such difference, however, result not only from the varied estimations in  
527 CPP emissions but also from discrepancy in other sources, e.g., intensive emissions  
528 from industrial sources in the area in AMAP/UNEP. For ISP and CEM, similarly,  
529 higher emissions were estimated by the provincial inventory for areas with big plants  
530 in Zhenjiang, Suzhou and Changzhou in southern Jiangsu. In contrast to the provincial  
531 inventory, that investigated the activities of each manufacturing processes, for  
532 individual plants, the emissions in national inventories (THU and NJU) were allocated  
533 based only on the production of plants, ignoring the effects of manufacturing  
534 technologies on emissions. Moreover, some CEM and ISP plants were missed in those  
535 national inventories, leading to underestimation in emissions for corresponding  
536 regions. When the national inventory was applied in CTM, the simulated  
537 concentrations of  $Hg^T$  were usually lower than the observation at rural sites in eastern  
538 China (Wang et al., 2014). Since many big plants are being moved from urban to rural  
539 areas (Zhao et al., 2015b; Zhou et al., 2016), improvement in model performance  
540 could be expected when the elevated emissions in rural areas are estimated and used  
541 for CTM, incorporating the accurate information of individual big plants.

542 With much fewer big emitters, discrepancies in gridded emissions for other part  
543 of Jiangsu resulted largely from the allocation of emissions as area sources in national  
544 and global inventories. For example, in spite of an estimation of 8496 kg smaller than  
545 the provincial inventory in total emissions, NJU inventory applied proxies (e.g.,  
546 population and GDP) to allocate the emissions except those from CPP, resulting in  
547 higher emissions in central and most part of northern Jiangsu (Figure 4(a)). Similar  
548 patterns are also found for THU (Figure 4(b)) and AMAP/UNEP (Figure 4(c))  
549 compared to provincial inventory.

550 Besides the total emissions, differences in spatial distribution of speciated Hg  
551 emissions between multi-scale inventories are presented in Figure S3 in the  
552 supplement. The various patterns for species are largely influenced by the distribution  
553 of different types of big point sources, as the speciation profiles vary significantly

删除的内容: , as described in Section 2,

删除的内容: for

删除的内容: were investigated

删除的内容: and the information is taken into consideration in emission estimation. In contrast,

删除的内容: individual

删除的内容: in national inventories (THU and NJU)

删除的内容: thus

删除的内容: were ignored

删除的内容: In general, due to lack of plant-specific information, previous inventories failed to capture the relatively large emissions from big point sources.

删除的内容: commonly

删除的内容: in preparation

删除的内容: considerable

554 between source types in the national and provincial inventories (Table 2). Compared  
555 to other inventories, larger  $Hg^0$  emissions were found in the provincial inventory in  
556 southern Jiangsu (particularly Zhenjiang and Taizhou) where CPPs with large fraction  
557 of  $Hg^0$  are intensively located. Elevated  $Hg^{2+}$  emissions were dominated by intensive  
558 CEM industry in Changzhou, Wuxi and Zhenjiang in southern Jiangsu, as the  $Hg^{2+}$   
559 fraction of CEM reaches 73% in the provincial inventory. Differences in  $Hg^p$   
560 emissions between inventories in central Jiangsu are closely related with the locations  
561 of OIB plants, attributed mainly to the relatively poor understanding of the particle  
562 control and thereby  $Hg^p$  release of OIB. The emissions in the provincial inventory is  
563 larger than THU but smaller than AMAP/UNEP, as the  $Hg^p$  mass fraction of OIB was  
564 assumed at 2% in THU while it reached 10% in AMAP/UNEP (Table 2).

删除的内容: that have

删除的内容: In contrast to  $Hg^0$  and  $Hg^{2+}$ , d

565 The vertical distribution of Hg releases, which is crucial for the transport range  
566 of atmospheric Hg, is also analyzed. Four groups of release height are defined: 0-58m,  
567 58-141m, 141-250m and >250m. Based on the detailed information of emission  
568 sources, the fractions of Hg releases into the four groups for CPP are 2%, 66%, 31%,  
569 and 1%, respectively, and the analogue numbers for OIB, ISP, and CEM are 85%,  
570 13%, 2%, and 0%; 4%, 44%, 12%, and 4%; and 6%, 94%, 0%, and 0%, respectively.  
571 The release heights for rest sources are uniformly assumed at the range of 0-58m. As a  
572 result, the fractions of total Hg emissions in the four groups are estimated as 35%,  
573 53%, 11% and 1%. In AMAP/UNEP inventory, as a comparison, the fractions at the  
574 height of 0-50m, 50-150m and >150m were estimated at 23%, 53% and 24%  
575 respectively, with larger share in Hg emitted over 150m than that in our provincial  
576 inventory. The smaller fraction of Hg emissions under 150m and larger fraction of  
577  $Hg^{2+}$  as discussed in Section 3.2 in the provincial inventory are expected to result in  
578 more local deposition and less long-range transport compared to previous inventories  
579 when they are applied in CTM. The re-emissions of legacy Hg could then be  
580 enhanced and make a significant contribution to atmospheric Hg concentrations, as  
581 indicated by Zhu et al. (2012).

删除的内容: in this work

删除的内容: lower

删除的内容: higher

删除的内容: s

删除的内容: our

删除的内容: believed

删除的内容: lead to

删除的内容: export

删除的内容: .

删除的内容: emit

删除的内容: deposited

删除的内容: increase natural emissions which is consistent with the speculation

删除的内容: that natural emissions made a significant contribution to the elevated GEM concentrations in summer

### 583 3.4 Uncertainty of the provincial inventory

584 As summarized in Table 4, the uncertainties of speciated Hg emissions in the  
585 provincial inventory are estimated at -24%~+82% (95% confidence intervals (CI)  
586 around central estimates), -34%~+99%, -23%~+68%, and -34%~+270% for  $Hg^T$ ,  $Hg^0$ ,  
587  $Hg^{2+}$  and  $Hg^p$ , respectively. For comparison, the uncertainties of Jiangsu emissions

588 from major sectors including CPP, CEM, ISP and OIB in NJU inventory are  
589 recalculated following Zhao et al. (2015a) and provided in Table 4 as well. The  
590 uncertainties for major sources in the provincial inventory were smaller than those in  
591 NJU inventory, attributed largely to the bottom-up approach used in provincial  
592 inventory with more accurate information on activity levels and APCDs applications  
593 for individual plants of Category 1. In addition, with more field measurements on Hg  
594 contents in coal and limestone incorporated, the uncertainties of  $HgC_{raw}$  and  
595  $HgC_{Limestone}$  are significantly reduced, resulting from the mechanism of error  
596 compensation when  $HgC_{raw}$  of coals produced in different provinces are taken into  
597 account in the inter-provincial flow model for coal transport, and from the success in  
598 bootstrap simulation, respectively. As a result, the uncertainties of emissions from  
599 CPP, OIB and CEM are effectively reduced in the provincial inventory.

删除的内容: As can be seen, t

删除的内容: ful application

删除的内容: of

600 The parameters contributing most to uncertainties and their contributions to the  
601 variance of corresponding emission estimates are summarized by sector in Table S8 in  
602 the supplement. For CPP and OIB, parameters related to emission factors contribute  
603 most to the uncertainties of  $Hg^T$  emissions, including the  $HgC_{raw}$  in provinces with  
604 largest contribution to the input of coal consumed in Jiangsu (i.e., Shaanxi and Inner  
605 Mongolia), and the removal efficiencies ( $RE$ ) or release ratios ( $RR$ ) of Hg for typical  
606 APCD (ESP+FGD) and combustor type (grate boiler).  $HgC_{raw}$  of coals produced in  
607 Shaanxi and Inner Mongolia that collectively accounted for 34% of coal consumption  
608 in Jiangsu, contributed 26% and 18% to the uncertainties of Hg emissions for CPP,  
609 and 15% and 11% to those for OIB, respectively. It is thus essential to conduct  
610 systematic and synergetic measurements on  $HgC_{raw}$  in different regions (particularly  
611 those with large coal production) to constrain the uncertainties of Hg emission  
612 estimation for coal combustion sources, at both regional and national scales. Given  
613 the wide application of ESP+FGD in CPP (70% in coal consumption),  $RE_{ESP+FGD}$  is  
614 estimated to contribute 20% to Hg emissions from CPP. Local measurements on  $RE$  of  
615 typical APCDs, which have started in Jiangsu (JSEMC, 2013; Xie and Yi, 2014), are  
616 expected to potentially improve the Hg emission estimation at regional level.  
617 Although applied in 92% of OIB plants in Jiangsu, there are very few studies on Hg  
618 release rate of grate boiler, resulting in a contribution of 5% to the emission  
619 uncertainty. For CEM,  $HgC_{Limestone}$  dominates the uncertainties of Hg emissions, with  
620 the contribution estimated at 84%. Attributed to lack of detailed information,  
621 provincial average of  $HgC_{Limestone}$  with the lognormal distribution fitted through

622 bootstrap simulation based on available measurements (Figure S2 and Table S6) was  
623 uniformly applied for all the individual plants, leading to the enhanced contribution to  
624 the uncertainty. For ISP, *EF* of limestone and dolomite production contributes 60% to  
625 Hg emissions, as the process is estimated to account for 88% of emissions from the  
626 entire sector. In addition, *AL* from the biggest ISP factory, which accounted for 40%  
627 and 75% of pig iron and crude steel production for the whole province, respectively,  
628 contributes 24% to the total uncertainty of ISP sector. The result indicates a necessity  
629 of specific investigation on super emitters. For rest sources, MSWI, BIO and O&G are  
630 the biggest sources for Hg<sup>T</sup> emissions, and *EFs* of those types of sources thus  
631 contribute most to the emission uncertainty.

632 In most cases, parameters with big contribution to uncertainty of Hg<sup>T</sup> also play  
633 crucial roles in uncertainty of speciated emissions. Moreover, the speciation profiles  
634 for typical source types and APCDs are identified as key parameters to the  
635 uncertainties of speciated emissions as well. For example, the mass fraction of Hg<sup>2+</sup>  
636 from ESP+FGD, and that of Hg<sup>p</sup> from ESP are the biggest contributors to  
637 uncertainties of Hg<sup>2+</sup> and Hg<sup>p</sup> emissions from CPP, respectively. For OIB, the mass  
638 fraction of Hg<sup>p</sup> from sources without any control is much higher than those with  
639 APCDs (Table 3), thus it plays an important role in the emission uncertainty, with the  
640 contribution estimated at 35%. For CEM and ISP, studies on speciation profiles are  
641 limited so far, and the speciation profiles for DPT+DR and ISP plants contribute  
642 largely to uncertainties of speciated emissions.

643

#### 644 4 CONCLUSIONS

645 Taking Jiangsu province in China as an example, the discrepancies and their  
646 sources of atmospheric Hg emission estimations in multi-scale inventories applying  
647 varied methods and data are thoroughly analyzed. Using a bottom-up approach that  
648 integrates best available information of individual plants and most recent field  
649 measurements, the total Hg emissions in Jiangsu 2010 are estimated larger than any  
650 other national/global inventories. CPP, ISP, CEM and OIB collectively accounted for  
651 90% of the total emissions. Comparisons between available studies demonstrate that  
652 the information gaps of multi-scale inventories lead to big differences in Hg emission  
653 estimation. Discrepancies in emissions between inventories for the above-mentioned  
654 major sources come primarily from various data sources for activity levels, Hg

删除的内容: calculated at 39  
105 kg, and the

删除的内容: is

655 contents in coals and total abatement effects of APCDs. Notable increase in Hg<sup>2+</sup>  
656 emissions is estimated with the bottom-up approach compared to other global/national  
657 inventories, attributed mainly to the adoption of domestic measurement results with  
658 elevated mass fraction of Hg<sup>2+</sup> for CEM, ISP and MSWI. Inconsistent information of  
659 big point sources lead to large differences in spatial distribution of emissions between  
660 provincial and other inventories, particularly in southern and northwestern of the  
661 province where intensive coal combustion and industry are located. Improved  
662 estimates in emission level, speciation and spatial distribution are expected to better  
663 support the regional chemistry transport modeling of atmospheric Hg. Compared to  
664 the national inventory, uncertainties of Hg emissions are reduced in provincial  
665 inventory using the bottom-up approach.

删除的内容:

666 The method developed and demonstrated for Jiangsu could potentially be  
667 promoted to other provinces, particularly for those with intensive industrial plants. As  
668 estimated in this work, for example, cement and iron & steel industries were the two  
669 most important sectors of which the Hg emissions were significantly underestimated  
670 by previous inventories for Jiangsu. The underestimations came mainly from the  
671 ignorance of high Hg release ratio of precalciner technology with dust recycling, and  
672 application of relatively low emission factors for steel production. We could thus  
673 cautiously infer that Hg emissions might be underestimated for China's other regions  
674 with intensive cement and steel industries in previous inventories. For power plants  
675 and industrial boilers, however, the Hg emissions were influenced largely by Hg  
676 contents in coal and APCDs application. Whether the emissions of those sources were  
677 underestimated or not for other parts of the country could hardly be judged unless  
678 detailed information gets available for the regions. Extensive and dedicated  
679 measurements are urgently suggested on Hg contents in coal/limestone and removal  
680 efficiency of dominating APCDs to further improve the emission estimation at  
681 regional/local scales, and eventually for the whole country.

删除的内容: Extensive and dedicated measurements are urgently suggested on Hg contents in coal/limestone and removal efficiency of dominating APCDs to further improve the emission estimation at regional/local scales.

### 682

### 683 DATA ACCESS

684 The gridded Hg emissions for Jiangsu province 2010 at a horizontal resolution of  
685 0.05°×0.05° can be downloaded at <http://www.airqualitynju.com/En/Default>.

686

687

## ACKNOWLEDGEMENT

688 This work was sponsored by the Natural Science Foundation of China  
689 (41575142), Natural Science Foundation of Jiangsu (BK20140020), Jiangsu Science  
690 and Technology Support Program (SBE2014070918), and Special Research Program  
691 of Environmental Protection for Commonweal (201509004). We would like to  
692 acknowledge Hezhong Tian from Beijing Normal University and Simon Wilson from  
693 UNEP/AMAP Expert Group for the detailed information on national/global Hg  
694 emission inventories.

695

696

## REFERENCES

- 697 AMAP/UNEP: Technical Background Report to the Global Atmospheric Mercury  
698 Assessment, Arctic Monitoring and Assessment Programme, Oslo, Norway/UNEP  
699 Chemicals Branch, Geneva, Switzerland, 159 pp., 2008.
- 700 AMAP/UNEP: Technical Background Report for the Global Mercury Assessment,  
701 Arctic Monitoring and Assessment Programme, Oslo, Norway/UNEP Chemicals  
702 Branch, Geneva, Switzerland, 263 pp., 2013.
- 703 Best Available Techniques Reference Document (BREF) for Iron and Steel Production,  
704 Industrial Emissions Directive 2010/75/EU. (Integrated Pollution Prevention and  
705 Control), European Commission, March, 2012, online at:  
706 [http://eippcb.jrc.ec.europa.eu/reference/BREF/IS\\_Adopted\\_03\\_2012.pdf](http://eippcb.jrc.ec.europa.eu/reference/BREF/IS_Adopted_03_2012.pdf).
- 707 Chen, C., Wang, H. H., Zhang, W., Hu, D., Chen, L., Wang, X. J.: High-resolution  
708 inventory of mercury emissions from biomass burning in China for 2000-2010 and a  
709 projection for 2020, *J. Geophys. Res.*, 118, 12248-12256, 2013.
- 710 Chen, L., Liu, M., Fan, R., Ma, S., Xu, Z., Ren, M., He, Q.: Mercury speciation and  
711 emission from municipal solid waste incinerators in the Pearl River Delta, South  
712 China, *Sci. Total Environ.*, 447, 396–402, 2013.
- 713 China Cement Association (CCA) : China cement almanac, China Building Industry  
714 Press, 2011.
- 715 Fu, X. W., Feng, X. B., Sommar, J., Wang, S. F.: A review of studies on atmospheric  
716 mercury in China, *Sci. Total Environ.*, 421–422, 73–81, 2012.
- 717 Fu, X. W., Zhang, H., Lin, C. J., Feng, X. B., Zhou, L. X., Fang, S. X.: Correlation  
718 slopes of GEM / CO, GEM / CO<sub>2</sub>, and GEM / CH<sub>4</sub> and estimated mercury emissions

719 in China, South Asia, the Indochinese Peninsula, and Central Asia derived from  
720 observations in northwestern and southwestern China, *Atmos. Chem. Phys.*, 15,  
721 1013–1028, 2015.

722 European Environment Agency (EEA): EMEP/EEA air pollutant emission inventory  
723 guidebook 2009, Technical report No 9/2009, available online at:  
724 <http://www.eea.europa.eu/publications/emep-eea-emission-inventory-guidebook-2009>

725 European Environment Agency (EEA): EMEP/EEA air pollutant emission inventory  
726 guidebook 2013, available online at:  
727 <http://www.eea.europa.eu/publications/emep-eea-guidebook-2013>

728 Habashi, F.: Metallurgical plants: how mercury pollution is abated, *Environ. Sci.*  
729 *Technol.*, 12, 1372-1376, 1978.

730 He, Z. Q., Kan, Z. N., Qi, L. M., Han, X. F.: Analysis to mercury removal  
731 performance test of bag-type dust collector, *Inner Mongolia Electric Power*, 30 (1),  
732 0040-0042, 2012 (in Chinese).

733 Hu, D., Zhang, W., Chen, L., Ou, L. B., Tong, Y. D., Wei, W., Long, W. J., Wang, X.  
734 J.: Mercury emissions from waste combustion in China from 2004 to 2010, *Atmos.*  
735 *Environ.*, 62, 359–366, 2012.

736 Jiangsu Environment Monitoring Center (JSEMC): Research on mercury emissions in  
737 flue gas of coal-fired power plants in Jiangsu Province, Interim report, 2013 (in  
738 Chinese).

739 Li, W.: Characterization of Atmospheric Mercury Emissions from Coal-fired Power  
740 Plant and Cement Plant (Master Thesis), Xi'an University, Chongqing, China, 2011  
741 (in Chinese).

742 Lin, C. J., Pan, L., Streets, D. G., Shetty, SK., Jang, C., Feng, X., Chu, H. W., Ho, T.  
743 C.: Estimating mercury emission outflow from East Asia using CMAQ-Hg, *Atmos.*  
744 *Chem. Phys.*, 10(4), 1853-1864, 2010.

745 Muntean, M., Janssens-Maenhout, G., Song, S., Selin, N. E., Olivier, J. G. J.,  
746 Guizzardi, D., Maas, R., Dentener, F.: Trend analysis from 1970 to 2008 and model  
747 evaluation of EDGARv4 global gridded anthropogenic mercury emissions,  
748 *Sci. Total Environ.*, 494–495, 337–350, 2014.

749 Nriagu, J. O.: Global inventory of natural and anthropogenic emissions of trace metals  
750 to the atmosphere, *Nature*, 279, 409-411, 1979.

751 National Statistical Bureau of China (NSB): China Statistical Yearbook, China



752 Statistics Press, Beijing, 2011a.

753 National Statistical Bureau of China (NSB): China Energy Statistical Yearbook, China  
754 Statistics Press, Beijing, 2011b.

755 National Statistical Bureau of China (NSB): China Industry Economy Statistical  
756 Yearbook, China Statistics Press, Beijing, 2011c.

757 Nonferrous Metal Industry Association of China (NMIA): Yearbook of Nonferrous  
758 Metals Industry of China, China Statistics Press, Beijing, 2011.

759 Pacyna, E. G., Pacyna, J. M., Sundseth, K., Munthe, J., Kindbom, K., Wilson, S.,  
760 Steenhuisen, F., Maxson, P.: Global emission of mercury to the atmosphere from  
761 anthropogenic sources in 2005 and projections to 2020, *Atmos. Environ.*, 44,  
762 2487-2499, 2010.

763 Pacyna, J. M.: Estimation of the atmospheric emissions of trace elements from  
764 anthropogenic sources in Europe, *Atmos. Environ.*, 18, 41-50, 1984.

765 Pacyna, J. M., and Pacyna, E. G.: An assessment of global and regional emissions of  
766 trace metals to the atmosphere from anthropogenic sources worldwide, *Environ. Rev.*,  
767 9, 269–298, 2001.

768 Pirrone, N., Cinnirella, S., Feng, X., Finkelman, R. B., Friedli, H. R., Leaner, J.,  
769 Mason, R., Mukherjee, A. B., Stracher, G. B., Streets, D. G., Telmer, K.: Global  
770 mercury emissions to the atmosphere from anthropogenic and natural sources, *Atmos.*  
771 *Chem. Phys.*, 10, 5951-5964, 2010.

772 Pirrone, N., Mason, R. P. (Eds): Mercury fate and transport in the global atmosphere,  
773 Springer US., 2009.

774 Steenhuisen, F., Wilson, S. J.: Identifying and characterizing major emission point  
775 sources as a basis for geospatial distribution of mercury emissions inventories, *Atmos.*  
776 *Environ.*, 112, 167-177, 2015.

777 Streets, D. G., Devane, M. K., Lu, Z., Bond, T. C., Sunderland, E.M., and Jacob, D.J.:  
778 All-time releases of mercury to the atmosphere from human activities, *Environ. Sci.*  
779 *Technol.*, 45, 10485–10491, 2011.

780 Tang, S. L., Feng, X. B., Shang, L. H., Yan, H. Y., Hou, Y. M.: Mercury speciation and  
781 emissions in the flue gas of a small-scale coal-fired boiler in Guiyang, *Research of*  
782 *Environmental Sciences*, 17, 74-76, 2004 (in Chinese).

783 Tian, H. Z., Liu, K. Y., Zhou, J. R., Lu, L., Hao, J. M., Q, P. P., G, J. J., Zhu, C. Y.,  
784 Wang, K., Hua, S. B.: Atmospheric Emission Inventory of Hazardous Trace Elements  
785 from Chinas Coal-Fired Power Plants Temporal Trends and Spatial Variation  
786 Characteristics, *Environ. Sci. Technol.*, 48, 3575-3582, 2014.

787 Tian, H. Z., Wang, Y., Xue, Z. G., Cheng, K., Qu, Y. P., Chai, F. H., Hao, J. M.: Trend  
788 and characteristics of atmospheric emissions of Hg, As, and Se from coal combustion  
789 in China, 1980–2007, *Atmos. Chem. Phys.*, 10, 11905-11919, 2010.

790 Tian, H. Z., Zhu, C. Y., Gao, J. J., Cheng, K., Hao, J. M., Wang, K., Hua, S. B., Wang,  
791 Y., Zhou, J. R.: Quantitative assessment of atmospheric emissions of toxic heavy  
792 metals from anthropogenic sources in China: historical trend, spatial distribution,  
793 uncertainties, and control policies, *Atmos. Chem. Phys.*, 15, 10127-10147, 2015.

794 Timmermans, R. M. A., Denier van der Gon, H. A. C., Kuenen, J. J. P., Segers, A. J.,  
795 Honoré, C., Perrussel, O., Builtjes, P. J. H., Schaap, M.: Quantification of the urban  
796 air pollution increment and its dependency on the use of down-scaled and bottom-up  
797 city emission inventories, *Urban Climate*, 6, 44-62, 2013.

798 United Nations Environment Programme (UNEP): Toolkit for Identification and  
799 Quantification of Mercury Releases, UNEP Chemicals Branch, 2005.

800 United Nations Environment Programme (UNEP): Toolkit for Identification and  
801 Quantification of Mercury Releases, Revised Inventory Level 2 Report including  
802 Description of Mercury Source Characteristics, Version 1.1., January 2011, 2011a,  
803 available online at:  
804 [www.unep.org/hazardoussubstances/Portals/9/Mercury/Documents/Publications/Tool](http://www.unep.org/hazardoussubstances/Portals/9/Mercury/Documents/Publications/Toolkit/Hg%20Toolkit-Reference-Report-rev-Jan11.pdf)  
805 [kit/Hg%20Toolkit-Reference-Report-rev-Jan11.pdf](http://www.unep.org/hazardoussubstances/Portals/9/Mercury/Documents/Publications/Toolkit/Hg%20Toolkit-Reference-Report-rev-Jan11.pdf).

806 United Nations Environment Programme (UNEP): Reducing Mercury Emissions from  
807 Coal Combustion in the Energy Sector of China, Prepared for the Ministry of  
808 Environment Protection of China and UNEP Chemicals, Tsinghua University, Beijing,  
809 China, February 2011, 2011b, available online at:  
810 [www.unep.org/hazardoussubstances/Portals/9/Mercury/Documents/coal/FINAL%20C](http://www.unep.org/hazardoussubstances/Portals/9/Mercury/Documents/coal/FINAL%20Chinese_Coal%20Report%20-%202011%20March%202011.pdf)  
811 [hinese\\_Coal%20Report%20-%202011%20March%202011.pdf](http://www.unep.org/hazardoussubstances/Portals/9/Mercury/Documents/coal/FINAL%20Chinese_Coal%20Report%20-%202011%20March%202011.pdf).

812 US Environmental Protection Agency (EPA): US National Emission Inventory 2008  
813 version 2 (April 2012), 2012, available online at:  
814 [www.epa.gov/ttn/chief/net/2008inventory.htm](http://www.epa.gov/ttn/chief/net/2008inventory.htm).

815 US Geological Survey (USGS): Mercury content in coal mines in China (unpublished  
816 data), 2004.

817 Wang, Q. C., Shen, W. G., Ma, Z. W.: Estimation of Mercury Emission from Coal  
818 Combustion in China, *Environ. Sci. Technol.*, 34, 2711-2713, 2000.

819 Wang, L., Wang, S. X., Zhang, L., Wang, Y. X., Zhang, Y. X., Nielsen, C., McElroy,  
820 M. B., Hao, J. M.: Source apportionment of atmospheric mercury pollution in China  
821 using the GEOS-Chem model, *Environ. Pollut.*, 190(7), 166-175, 2014.

822 Wang, S. X., Zhang, L., Li, G. H., Wu, Y., Hao, J. M., Pirrone, N., Sprovieri, F.,  
823 Ancora, M. P.: Mercury emission and speciation of coal-fired power plants in China,  
824 *Atmos. Chem. Phys.*, 10, 1183-1192, 2010.

825 Wang, Y. J., Duan, Y. F., Yang, L. G., Jiang, Y. M., Wu, C. J., Wang, Q., Yang, X. H.:  
826 Analysis of the factors exercising an influence on the morphological transformation of  
827 mercury in the flue gas of a 600MW coal-fired power plant,  
828 *Journal of Engineering for Thermal Energy and Power*, 04, 399-403, 2008 (in  
829 Chinese).

830 Wang, F. Y., Wang S. X., Zhang, L., Yang, H., Gao, W., Wu, Q. R., Hao, J. M.:  
831 Mercury mass flow in iron and steel production process and its implications for  
832 mercury emission control, *Journal of Environmental Sciences*, 2016 (in press),  
833 available online at: <http://dx.doi.org/10.1016/j.jes.2015.07.019>.

834 Wu, Q. R., Wang, S. X., Zhang, L., Song, J. X., Yang, H., Meng, Y.: Update of  
835 mercury emissions from China's primary zinc, lead and copper smelters, 2000–2010,  
836 *Atmos. Chem. Phys.*, 12, 11153-11163, 2012.

837 Xie, X., Yin, W.: Nanjing Thermal Power Plant Boiler Flue Gas Mercury Emissions in  
838 the Survey, *Environmental Monitoring and Forewarning*, 6, 47-49, 2014.

839 Yang, H.: Study on atmospheric mercury emission and control strategies from cement  
840 production in China, M.S. thesis, Tsinghua University, Beijing, China, 2014 (in  
841 Chinese).

842 Yao, W., Qu, X. H., Li, H. X., Fu, Y. F.: Production, collection and treatment of  
843 garbage in rural areas in China, *Journal of Environment and Health*, 26, 10-12, 2009  
844 (in Chinese).

845 Zhang, L.: Emission Characteristics and Synergistic Control Strategies of

846 Atmospheric Mercury from Coal Combustion in China, Ph. D thesis, Tsinghua  
847 University, Beijing, China, 2012 (in Chinese).

848 Zhang, L.: Research on mercury emission measurement and estimate from  
849 combustion resources (Master Thesis), Zhejiang University, Hangzhou, China, 2007  
850 (in Chinese).

851 Zhang, L., Wang, S. X., Meng, Y., Hao, J. M.: Influence of mercury and chlorine  
852 content of coal on mercury emissions from coal-fired power plants in China, *Environ.*  
853 *Sci. Technol.*, 46, 6385-6392, 2012.

854 Zhang, L., Wang, S. X., Wang, L., Wu, Y., Duan, L., Wu, Q. R., Wang, F. Y., Yang, M.,  
855 Yang, H., Hao, J. M., Liu, X.: Updated Emission Inventories for Speciated  
856 Atmospheric Mercury from Anthropogenic Sources in China, *Environ. Sci. Technol.*,  
857 49, 3185–3194, 2015.

858 Zhao, Y., Wang, S. X., Duan, L., Lei, Y., Cao, P. F., Hao, J. M.: Primary air pollutant  
859 emissions of coal-fired power plants in China: current status and future prediction,  
860 *Atmos. Environ.*, 42, 8442-8452, 2008.

861 Zhao, Y., Nielsen, C. P., Lei, Y., McElroy, M. B., Hao, J. M.: Quantifying the  
862 uncertainties of a bottom-up emission inventory of anthropogenic atmospheric  
863 pollutants in China, *Atmos. Chem. Phys.*, 11, 2295-2308, 2011.

864 Zhao, Y., Nielsen, C. P., McElroy, M. B., Zhang, L., Zhang, J.: CO emissions in  
865 China: uncertainties and implications of improved energy efficiency and emission  
866 control, *Atmos. Environ.*, 49, 103-113, 2012.

867 Zhao, Y., Zhong, H., Zhang, J., Nielsen, C. P.: Evaluating the effects of China's  
868 pollution controls on inter-annual trends and uncertainties of atmospheric mercury  
869 emissions, *Atmos. Chem. Phys.*, 15, 4317-4337, 2015a.

870 Zhao, Y., Qiu, L. P., Xu, R. Y., Xie, F. J., Zhang, Q., Yu, Y. Y., Nielsen, C. P., Qin,  
871 H. X., Wang, H. K., Wu, X. C., Li, W. Q., Zhang, J.: Advantages of a city-scale  
872 emission inventory for urban air quality research and policy: the case of Nanjing, a  
873 typical industrial city in the Yangtze River Delta, China, *Atmos. Chem. Phys.*, 15,  
874 18691-18746, 2015b.

875 Zhou, Y., Zhao, Y., Mao, P., Zhang, Q., Zhang, J., Qiu, L., Yang, Y.: Development of  
876 a high-resolution emission inventory and its evaluation through air quality modeling

877 | for Jiangsu Province, China, [Atmos. Chem. Phys. Discuss.](https://doi.org/10.5194/acp-2016-567), doi:10.5194/acp-2016-567,  
878 | 2016.

879 | Zhu, J., Wang, T. J., Bieser, J., Matthias, V.: Source attribution and process analysis  
880 | for atmospheric mercury in East China simulated by CMAQ-Hg, *Atmos. Chem. Phys.*,  
881 | 15, 8767-8779, 2015.

882 | Zhu, J., Wang, T. J., Talbot, R., Mao, H.: Characteristics of atmospheric total gaseous  
883 | mercury (tgm) observed in urban Nanjing, China, *Atmos. Chem. Phys.*, 12,  
884 | 25037-25080, 2012.

删除的内容: (in preparation)

**TABLES**

**Table 1 Emission estimates for Jiangsu in 2010 and species from multi-scale inventories by sector. Recall from Section 2 the abbreviations for emission sources: CPP: coal-fired power plants; RCC: residential coal combustion; O&G: oil and gas combustion; OIB: other industrial coal combustion; CEM: cement production; ISP: iron & steel plants; NMS: nonferrous metal smelting; AP: aluminum production; LGM: large-scale gold mining; MM: mercury mining; HC: human cremation; MSWI: municipal solid waste incineration; RSWI: rural solid waste incineration; BFLP: battery/fluorescent lamp production; BIO: biofuel use/biomass open burning; and PVC: PVC production.**

		CPP <sup>1</sup>	RCC <sup>3</sup>	O&G <sup>3</sup>	OIB <sup>1</sup>	CEM <sup>1</sup>	ISP <sup>1</sup>	NMS <sup>2</sup>	AP <sup>2</sup>	LGM	MM	HC <sup>3</sup>	MSWI <sup>2</sup>	RSWI <sup>3</sup>	BFLP <sup>2</sup>	BIO <sup>3</sup>	PVC <sup>2</sup>	Total	
Hg <sup>T</sup>	Bottom-up	11549	195	930	8652	9264	5654	91	29	0	0	326	1009	365	158	461	423	39106	
	NJU	11208	165	930	6901	1137	2243	2158	/	23	51	/	1009	457	1225	500	2603	30610	
	THU	10768	345	752	10680	8238	2539	0	29	0	0	326	2294		244	219	/	36434	
	BNU	12883	267	898	10172	3288	2669	2022	6		/		308			303	/	32816	
	AMAP/UNEP		9292 <sup>a</sup>					17759 <sup>b</sup>						4976 <sup>c</sup>			/		32027
	EDGARv4.tox2	10233 <sup>d</sup>	1181 <sup>c</sup>	/	3310 <sup>f</sup>	6364	447	413		/			1017		/	43	/		23008
Hg <sup>0</sup>	Bottom-up	8811	91	465	4689	2461	1908	45	23	0	0	313	1017	47	158	350	423	20801	
	NJU	8133	42	465	2042	685	1208	1189	/	16	41	/	190		980	380	2082	17453	
	THU	7689	247	376	6995	2793	863	0	23	0	0	313	2202		244	162	/	21907	
	AMAP/UNEP		4646 <sup>a</sup>					14207 <sup>b</sup>						4668 <sup>c</sup>			/		23521
Hg <sup>2+</sup>	Bottom-up	2653	73	372	3394	6752	3746	45	4	0	0	0	868	314	0	23	0	18244	
	NJU	2900	45	372	4003	431	835	963	/	7	8	/	868	59	184	25	390	11090	
	THU	3058	92	301	3471	5338	1676	0	4	0	0	0	0		0	11	/	13951	
	AMAP/UNEP		3717 <sup>a</sup>					2707 <sup>b</sup>						238 <sup>c</sup>			/		6662
Hg <sup>p</sup>	Bottom-up	85	32	93	569	51	0	0	1	0	0	13	10	4	0	88	0	946	
	NJU	175	79	93	855	20	200	6	/	0	3	/	10	5	61	95	130	1732	
	THU	22	6	75	214	107	0	0	1	0	0	13	92		0	46	/	576	
	AMAP/UNEP		929 <sup>a</sup>					845 <sup>b</sup>						70 <sup>c</sup>			/		1844

<sup>1,2,3</sup> Sectors in category 1, 2 and 3 as classified in Section 2. <sup>a</sup> Stationary combustion sources: power plants, distributed heating, and other energy use (industrial sources excluded). <sup>b</sup> Industrial sources including stationary combustion for industry, CEM, ISP, NMS, AP, LGM and MM. <sup>c</sup> Intentional use and product waste associated sources: artisanal and small-scale gold mining, solid waste incineration and other product waste disposal, chlor-alkali industry, and human cremations. <sup>d,e,f</sup> Both coal and other fossil fuel combustion included.

**Table 2 Hg speciation profiles by sector and the mass fractions to total emissions in multi-scale inventories (%).**

Sector	Provincial inventory			NJU			THU			AMAP/UNEP		
	Hg <sup>0</sup>	Hg <sup>2+</sup>	Hg <sup>p</sup>	Hg <sup>0</sup>	Hg <sup>2+</sup>	Hg <sup>p</sup>	Hg <sup>0</sup>	Hg <sup>2+</sup>	Hg <sup>p</sup>	Hg <sup>0</sup>	Hg <sup>2+</sup>	Hg <sup>p</sup>
CPP	76	23	1	73	26	2	71	28	0	50	40	10
RCC	46	37	16	25	27	48	71	27	2	50	40	10
O&G	50	40	10	50	40	10	50	40	10	50	40	10
OIB	54	39	7	30	57	13	66	33	2	50	40	10
CEM	27	73	1	60	38	2	34	65	1	80	15	5
ISP	34	66	0	54	37	9	34	66	0	80	15	5
NMS	50	50	0	55	45	0		/		80	15	5
AP	80	15	5		/		80	15	5	80	15	5
LGM				70	30	0				80	15	5
MM		/		80	15	5		/		80	20	0
ASGM					/					100	0	0
HC	96	0	4				96	0	4	80	15	5
MSWI	13	86	1	13	86	1	96	0	4	20	60	20
BFLP	100	0	0	80	15	5	100	0	0	80	15	5
BIO	76	5	19	76	5	19	74	5	21		/	
PVC	100	0	0	80	15	5		/				
Total	51	47	2	57	37	6	60	38	2	73	21	6

**Table 3 Hg speciation profiles used in provincial and national inventories for typical APCDs (%).**

Sources	Hg speciation									
	Provincial inventory			NJU			THU			
	Hg <sup>0</sup>	Hg <sup>2+</sup>	Hg <sup>p</sup>	Hg <sup>0</sup>	Hg <sup>2+</sup>	Hg <sup>p</sup>	Hg <sup>0</sup>	Hg <sup>2+</sup>	Hg <sup>p</sup>	
Coal combustion	ESP	57	41	1	65	35	0	58	41	1
	FF	31	61	7	16	73	11	50	49	1
	WET	65	33	2	30	57	13	65	33	2
	CYC	30	57	14	30	57	13		/	
	ESP+FGD	83	16	0	83	16	0	84	16	1
	SCR+ESP+FGD	71	29	0	72	28	0	74	26	0
	FF+FGD	78	21	1		/		78	21	1
	No	48	34	18	24	20	56	56	34	10
CEM	DPT+DR/FF*	24	75	1	16	73	11	24	76	1
	SKT/ESP*	83	16	1	65	35	0	80	15	5
	RKT/WET*	47	51	1	30	57	14	80	15	5

\*: DPT+DR, SKT and RKT for provincial and THU inventory (Zhang et al., 2015); FF, ESP and WET for NJU inventory (Zhao et al., 2015).



**Table 4. Uncertainties of Hg emissions in Jiangsu in provincial and national (NJU) inventories by source, expressed as the 95% confidence intervals of central estimates.**

Sources		Hg <sup>T</sup>	Hg <sup>0</sup>	Hg <sup>2+</sup>	Hg <sup>P</sup>
Provincial	CPP	(-59%, +147%)	(-64%, +131%)	(-56%, +244%)	(-43%, +418%)
	CEM	(-15%, +58%)	(-36%, +87%)	(-18%, +63%)	(-57%, +218%)
	ISP	(-38%, +53%)	(-33%, +156%)	(-62%, +44%)	/
	OIB	(-52%, +138%)	(-55%, +133%)	(-55%, +146%)	(-67%, +329%)
	Rest sources	(-25%, +133%)	(-20%, +151%)	(-67%, +168%)	(-43%, +367%)
	Total	(-26%, +81%)	(-34%, +99%)	(-23%, +68%)	(-34%, +270%)
NJU	CPP	(-80%, +198%)	(-80%, +198%)	(-80%, +201%)	(-75%, +477%)
	CEM	(-62%, +97%)	(-75%, +140%)	(-63%, +82%)	(-73%, +266%)
	ISP	(-81%, +167%)	(-82%, +157%)	(-82%, +170%)	(-81%, +250%)
	OIB	(-83%, +153%)	(-97%, +218%)	(-97%, +228%)	(-87%, +170%)

## FIGURES

**Fig. 1.** The ratios of estimated Hg emissions for Jiangsu 2010 in global/national inventories to that in provincial inventory for selected sources and anthropogenic total.

**Fig. 2.** Sensitivity analysis of selected parameters in Hg emission estimation for Category 1 sources. (a) Relative changes in parameters, calculated using Eq. (6); (b) Changes in emissions when parameters in the provincial inventory were replaced with those in other inventories, calculated using Eq. (7).  $HgC_{raw}$ : Hg content in raw coal; AL: activity levels as raw coal consumption by CPP and OIB, limestone used by CEM, and crude steel produced in ISP; TA: total abatement rate of APCDs; RR: Hg release rate for combustion; IEF: input emission factors (before control of APCDs); UEF: uniform emission factor (without consideration of different APCD types);  $EF_{iron}$  and  $EF_{steel}$ : emission factors of pig-iron and steel production respectively.

**Fig. 3.** Spatial distribution of Hg emissions for Jiangsu 2010 at a resolution of  $0.05^{\circ} \times 0.05^{\circ}$  for (a)  $Hg^T$ , (b)  $Hg^0$ , (c)  $Hg^{2+}$ , and (d)  $Hg^p$ .

**Fig. 4.** Differences in gridded  $Hg^T$  emissions in Jiangsu 2010 between provincial and other inventories: emissions in provincial inventory minus those in NJU (a), THU (b), AMAP/UNEP (c) and EDGARv4.tox2 (d). The locations of point sources with relatively large Hg emissions estimated in provincial inventory are indicated in the panels as well.

**Fig. 1**

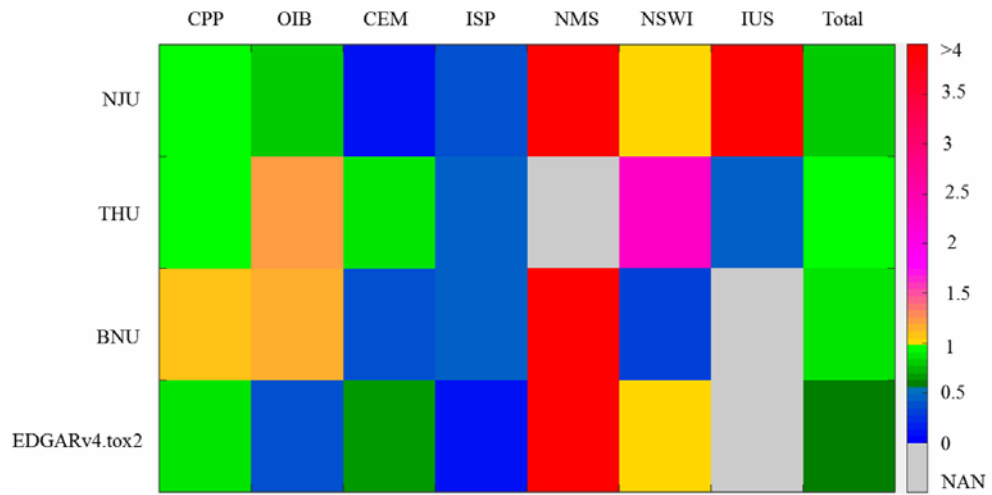


**Fig. 2.**

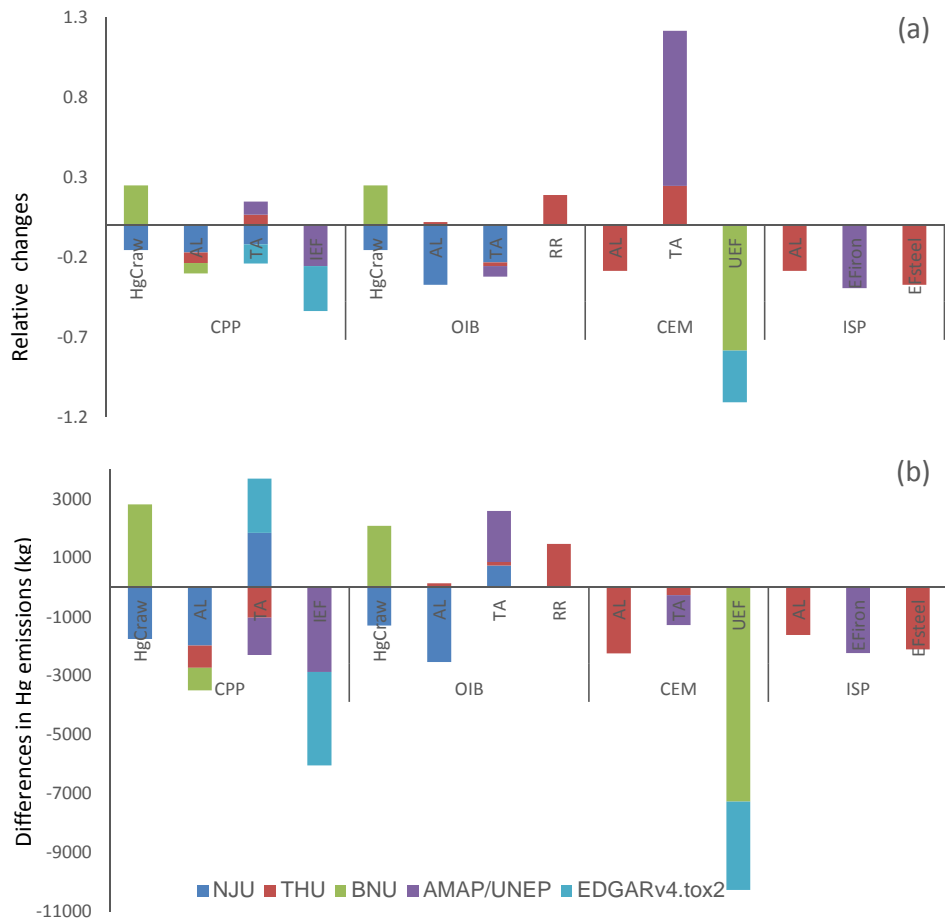


**Fig. 3.**

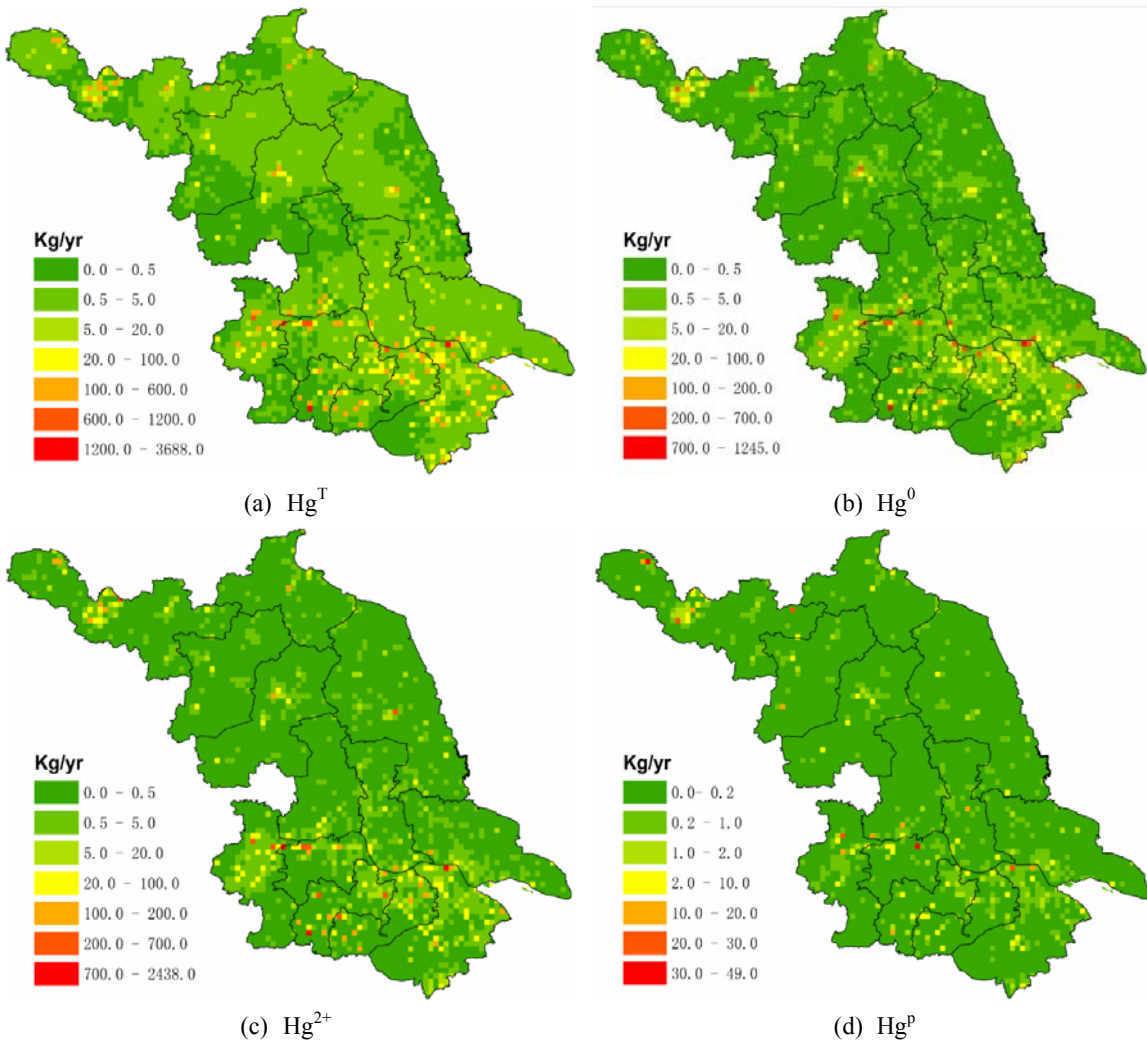
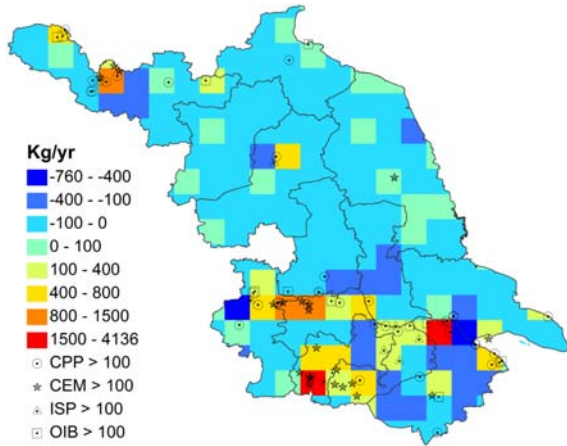
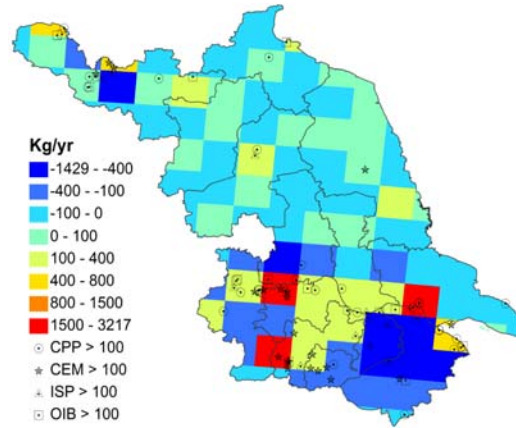


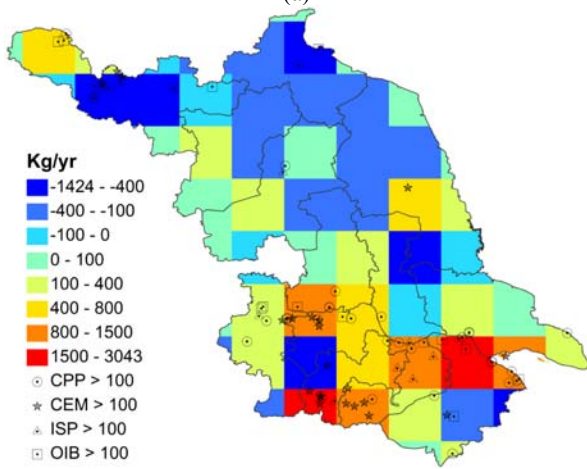
**Fig. 4.**



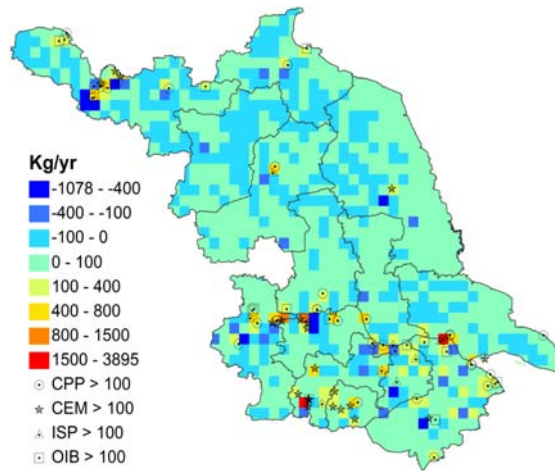
(a)



(b)



(c)



(d)